IAEA-TECDOC-1203

Thermohydraulic relationships for advanced water cooled reactors

INTERNATIONAL ATOMIC ENERGY AGENCY IAEA

April 2001

Chapter 3

A GENERAL CHF PREDICTION METHOD FOR ADVANCED WATER COOLED REACTORS

NOMENCLATURE

C	Constant	-
CHF	Critical heat flux	kW/m^2
Cp	Specific heat	kJ/(kg °C)
De, D_{hy}	Hydraulic equivalent diameter	m
D_{he}	Heated equivalent diameter	m
D	Tube inside diameter	m
d	Fuel element diameter	m
E	Entrainment rate	$kg/(m^2 s)$
g	Acceleration due to gravity	m/s^2
G	Mass flux	$kg/(m^2 s)$
H	Enthalpy	kJ/kg
h	Heat transfer coefficient k	$W/(m^2 °C)$
K, F	Correction factor	-
L_{sp}	Distance to upstream spacer plane	m
L	Heated length	m
P	Pressure	kPa
p	Element pitch	m
q	Surface heat flux	kW/m^2
T	Temperature	°C
U	Velocity	m/s
X	Quality	-
Z	Axial co-ordinate	m

GREEK SYMBOLS

α	Void fraction	-
δ	Inter element gap	m
ϕ	Surface heat flux	kW/m^2
λ	Latent heat of evaporation	kJ/kg
ρ	Density	kg/m^3
σ	Surface tension	N/m
y	Dimensionless mass flux	-
ΔH	Local subcooling, $h_s - h$	kJ/kg
ΔX	Bundle quality imbalance	-
ΔT	Local subcooling, $T_s - T$	°C
θ	Angle	degrees

SUBSCRIPTS

a	Actual value
avg	Average value
b	Bubble, bulk, boiling
BLA	Boiling length average

c	Critical, convection
CHF	Critical heat flux
DO	Dryout
f	Saturated liquid value
fg	Difference between saturated vapour and saturated liquid value
h, H	Heated
hom	Homogeneous
g	Saturated vapour
I, in	Inside, inlet
l	Liquid
m	Maximum
max.	Maximum
min	Minimum
nu	Non-uniform AFD
P/B	Pool boiling
o	Outside, outlet
rad	Radiation
s	Saturation value
sub	Subcooling
U	Uniform (AFD)
v	Vapour

ABBREVIATIONS

AFD	Axial flux distribution
BLA	Boiling length average
CHF	Critical heat flux
c/s	Cross section
DNB	Departure from nucleate boiling
DO	Dryout
FB	Film boiling
PDO	Post-dryout
RFD	Radial flux distribution

3.1. INTRODUCTION

The objective of this chapter is to recommend a validated CHF prediction method suitable for the assessment of critical power at both normal operating conditions and accident conditions in Advanced Water Cooled Reactors (AWCRs). This method can be implemented into systems codes such as RELAP, CATHARE, CATHENA as well as subchannel codes such as COBRA, ASSERT and ANTEO. The requirement of this prediction method has been discussed in more detail in previous CRP RCM meetings and expert meetings.

The two main applications for CHF predictions are:

(i) to set the operating power with a comfortable margin to avoid CHF occurrence. This margin to CHF can be expressed in terms of Minimum Critical Heat Flux Ratio (MCHFR, ratio of CHF to local heat flux for the same pressure, mass flux and quality), Minimum Critical Heat Flux Power Ratio (MCHFPR, the ratio of power at initial CHF occurrence to the operating power for the same pressure mass

flux and inlet temperature), or Minimum Critical Power Ratio (MCPR, the ratio of reactor or fuel channel power at initial dryout occurrence to normal operating power for the same system, pressure and inlet temperature); the definition of these ratios is illustrated in Fig. 3.1. A detailed discussion has been provided by Groeneveld (1996). Most CHF prediction methods address this concern; these prediction methods provide best-estimate values of the *initial CHF* occurrence in a reactor core or fuel bundle.

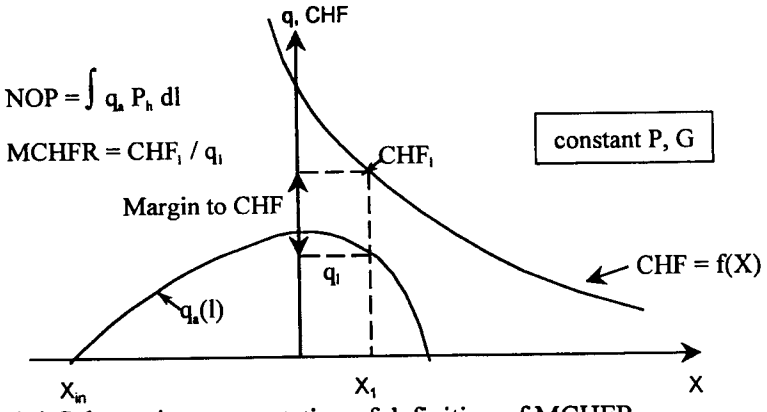

(a) Schematic representation of definition of MCHFR

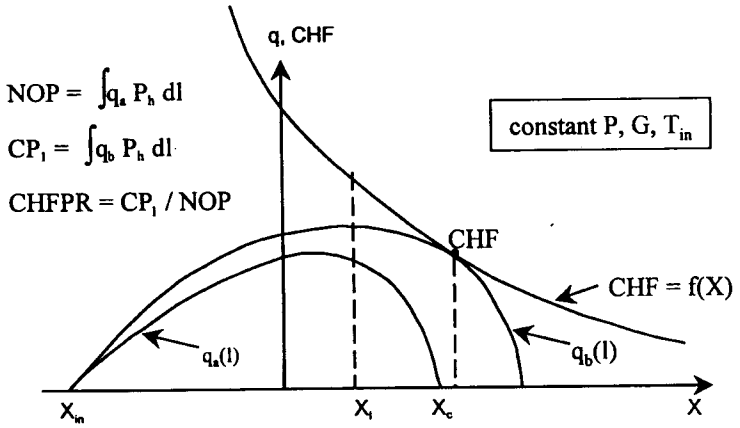

(b) Schematic representation of definition of MCHFPR

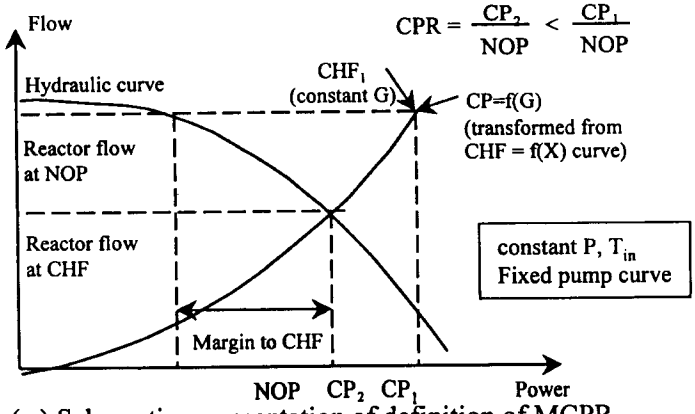

(c) Schematic representation of definition of MCPR

FIG. 3.1. Definition of margins to CHF as defined by MCHFR, MCHFPR and MCPR.

(ii) to evaluate the thermalhydraulic and neutronic response to CHF occurrence in a reactor core. This requires knowledge of how CHF spreads in the reactor core, which in turn requires a best-estimate prediction of the *average CHF* for a section of the core and/or prediction of the variation of fuel surface area in dryout as a function of power.

This chapter is subdivided as follows: Section 3.2 discusses various CHF mechanisms, followed by a description of the CHF database in Section 3.3. In Section 3.4, CHF prediction methodologies are reviewed for both tubes and bundle geometries, ranging from correlations, subchannel codes, analytical models and look up tables. In Section 3.5, the recommended prediction methods for CHF in AWCRs are described, together with correction factors to account for various CHF separate effects. The assessment of the accuracy of the recommended prediction method when applied to steady state conditions is described in Section 3.6. Finally in Section 3.7 the prediction of CHF during transients such as LOCAs, flow and power transients are discussed.

The topic of CHF has been extensively researched during the past 30 years. Excellent reviews may be found in text books by Collier (1981), Tong (1965), Tong and Weisman (1996), Hewitt (1970) and Hetsroni (1982), and review articles by Bergles (1977), Tong (1972), Groeneveld and Snoek (1986), Weisman (1992) and Katto (1994).

3.2. CHF MECHANISMS

3.2.1. General

In forced convective boiling, the boiling crisis[2] occurs when the heat flux is raised to such a high level that the heated surface can no longer support continuous liquid contact. This heat flux is usually referred to as the critical heat flux (CHF). It is characterized either by a sudden rise in surface temperature caused by blanketing of the heated surface by a stable vapour layer, or by small surface temperature spikes corresponding to the appearance and disappearance of dry patches. The CHF normally limits the amount of power transferred, both in nuclear fuel bundles, and in conventional boilers. Failure of the heated surface may occur once the CHF is exceeded. This is especially true for highly subcooled CHF conditions. At high flows and positive dryout qualities, the post-dryout heat transfer is reasonably effective in keeping the heated surface temperatures at moderate levels, and operation in dryout may be sustained safely for some time.

In flow boiling the CHF mechanisms depend on the flow regimes and phase distributions, which in turn are controlled by pressure, mass flux and quality. For reactor conditions of interest, the flow quality generally has the strongest effect on CHF: the CHF decreases rapidly with an increase in quality. The change in CHF with pressure, mass flux and quality is illustrated in the tables of Appendix II. The following sections describe the CHF mechanisms encountered at different qualities and flow conditions.

3.2.2. DNB (departure from nucleate boiling)

(i) *Nucleation induced.* This type of CHF is encountered at high subcooling (negative flow qualities) where heat is transferred very efficiently by nucleate boiling. Here the bubbles grow and collapse at the wall; between the bubbles some convection will take place.

[2] Other terms used to denote the boiling crisis: burnout, dryout, departure from nucleate boiling (DNB).

The CHF (or DNB) occurs at very high surface heat fluxes. It has been suggested [Collier (1981); Tong (1972)] that the CHF occurrence is due to the spreading of a drypatch following microlayer evaporation under a bubble and coalescence of adjacent bubbles although no definite proof of this is yet available. The occurrence of CHF here only depends on the local surface heat flux and flow conditions and is not affected by the upstream heat flux distribution. The surface temperature excursion occurring once CHF is exceeded is very rapid (fast dryout) and usually results in a failure of the heated surface.

(ii) *Bubble clouding.* In subcooled and saturated nucleate boiling (approximate quality range: from –5% to +5%) the number of bubbles generated depends on the heat flux and bulk temperature. The bubble population density near the heated surface increases with increasing heat flux and a so-called bubble boundary layer [Tong (1965), Weismann (1983)] often forms a short distance away from the surface. If this layer is sufficiently thick it can impede the flow of coolant to the heated surface. This in turn leads to a further increase in bubble population until the wall becomes so hot that a vapour patch forms over the heated surface. This type of boiling crisis is also characterized by a fast rise of the heated surface temperature (fast dryout). Physical failure of the heated surface frequently occurs under these conditions.

3.2.3. Helmholtz instability

In saturated pool boiling, the CHF is limited by the maximum vapour removal rate. Zuber's theory of CHF [as reported by Hsu and Graham (1976)] assumes the heated surface to be covered by a rising vapour column with countercurrent liquid jets flowing downwards to compensate for the removal of liquid by evaporation. Ultimately at very high heat flux levels (vapour removal rates) the relative velocity between liquid and vapour will be so high that an unstable flow situation is created, resulting in a CHF condition. This was recognized by Kutateladze (1952) who based his hydrodynamic theory of the boiling crisis on this instability. A similar situation can be considered at very low flow rates or flow stagnation conditions. This type of CHF is accompanied by a rapid rise in surface temperature (fast dryout).

3.2.4. Annular film dryout

In the annular dispersed flow regime (high void fraction and mass flow) the liquid will be in the form of a liquid film covering the walls and entrained droplets moving at a higher velocity in the core. Continuous thinning of the liquid film will take place due to the combined effect of entrainment and evaporation. Near the dryout location the liquid film becomes very thin and due to the lack of roll waves (which normally occur at higher liquid film flow rates) entrainment is suppressed. If the net droplet deposition rate does not balance the evaporation rate the liquid film must break down. The temperature rise accompanying this film breakdown is usually moderate (stable dryout). The liquid film breakdown may be promoted by one of the following mechanisms:

(i) *Thermocapillary effect:* If a significant amount of heat is transferred by conduction through the liquid film and the interface is wavy, the temperature of the liquid vapour interface will have a maximum in the valley of the wave and large surface tension gradients will be present. The surface tension gradients tend to draw liquid to areas of high surface tension. Under influence of this "thermocapillary effect" the liquid film

will eventually break down in the valley of the wave. This mechanism is thought to be important at low flows and high qualities.

(ii) *Nucleation induced film breakdown:* Hewitt et al. (1963) noticed that nucleation and surface evaporation could occur simultaneously in the annular flow regime. If the liquid film thickness is close to the maximum bubble size, then the bubble may rupture the liquid vapour interface and a momentary drypatch could occur. At high heat flux levels the liquid film may be prevented from rewetting this spot by the high drypatch temperatures. This mechanism will only occur for local heat flux spikes, or a highly non-uniform axial heat flux distribution.

3.2.5. Unstable or periodic dryout

The critical heat flux can be considerably reduced due to the hydrodynamic characteristics of the experimental equipment. Flow oscillations are frequently encountered in parallel channels, channels experiencing slug flow or in systems having a compressible volume near the inlet. During an oscillation the velocity at the wall is periodically slowed down, thus permitting the boundary layer to become superheated which may lead to a premature formation of a drypatch. Unstable dryouts are accompanied by an oscillation in surface temperature.

3.2.6. Slow dryout

During a slow dryout the heated surface does not experience the usual dryout temperature excursions; instead, a gradual increase in surface temperature with power is observed. A slow dryout is usually encountered in flow regimes where the phases are distributed homogeneously such as froth flow or highly dispersed annular flow at high mass velocities (>2.7 Mg m^{-2} s^{-1}) and void fractions >80%. At these conditions liquid-wall interaction is significant thus limiting the temperature rise at dryout. Calculations based on cooling by the vapour flow only indicate that post-CHF temperatures are below the minimum film boiling (Leidenfrost) temperature; hence depositing droplets may wet the surface thus increasing the heat transfer coefficient.

3.3. CHF DATABASE

3.3.1. General

Since the CHF usually limits the power output in water cooled reactors, accurate values of CHF are required. The CHF has been measured extensively in simple geometries such as directly heated tubes. Such measurements have helped us to understand the CHF mechanisms. However to obtain accurate values of the CHF at reactor conditions of interest, experiments in test sections closely simulating the reactor fuel bundles are required. Such experiments are very expensive; e.g., CHF tests in Canada alone have cost over 30 million dollars over the past 20 years.

To reduce the expense and complexity of CHF testing of full-scale fuel bundles with high pressure steam-water, low-latent-heat modeling fluids have been used. Freons have been used successfully in many heat transfer laboratories as a modeling fluid for simulating the CHF of water. Reliable CHF predictions for water can be made based on CHF measurements in Freons at considerably lower pressures (e.g. 1.56 MPa in Freon-12 compared to 10 MPa in water), temperatures (e.g. 50°C in Freon-12 compared to 300°C in water) and powers (e.g.

685 kW in Freon-12 compared to 10 MW in water), resulting in cost savings of around 80% compared to equivalent experiments in water.

In Sections 3.3.2 and Section 3.3.3, the available databases will be discussed. Particular attention is given to the CHF data in tubes as:

(i) the tube database is most complete and covers a much wider range of flow conditions than any other geometry, and
(ii) bundle geometries can be broken down into subchannels (see Section 3.4.4) which are traditionally assumed to behave as tubes with correction factors applied to account for subchannel specific effects.

TABLE 3.1. RANGES OF CONDITIONS COVERED BY VARIOUS SETS IN THE AECL DATABANK

References	Diameter (mm)	Length (m)	Pressure (MPa)	Mass Flux ($Mg.m^{-2}.s^{-1}$)	Dryout Quality (–)	Inlet Subcooling ($kJ.kg^{-1}$)	Critical Heat Flux ($MW.m^{-2}$)	No. of Data
Alekseev [Kirillov, 1992]	10.0	1.000–4.966	9.80–19.6	0.216–7.566	–0.866–0.944	57–1398	0.134–4.949	1108
Becker et al. [1962, 1963]	3.94–20.1	0.400–3.750	0.22–8.97	0.100–3.183	–0.069–1.054	–50–1640	0.278–7.477	2664
Becker et al. [1965]	3.93–37.5	0.216–3.750	1.13–9.91	0.160–5.586	–0.005–0.993	–16–2711	0.503–6.620	1343
Becker and Ling [1970]	2.40–36.0	0.500–1.880	3.05–7.10	0.093–2.725	0.207–0.903	371–1065	1.026–5.130	116
Becker et al. [1971]	10.0	1.000–4.966	3.00–20.0	0.156–8.111	–0.866–1.061	26–1414	0.135–5.476	1496
Bennett et al. [1965]	9.22–12.6	1.524–5.563	6.61–7.48	0.624–5.844	0.026–0.948	21–691	0.590–3.300	201
Bergelson [1980]	8.00	0.241–0.400	0.17–3.08	1.927–7.078	–0.295–0.090	96–853	3.511–14.57	336
Bergles [1963]	0.62–6.21	0.011–0.155	0.14–0.59	1.519–24.27	–0.137–0.111	25–534	4.957–44.71	117
Bertoletti et al. [1964]	4.90–15.2	0.050–2.675	4.88–9.88	1.051–3.949	–0.083–0.774	–28–769	0.199–7.503	386
Borodin and MacDonald [1984]	8.92	3.690–3.990	8.20–10.4	1.194–6.927	0.105–0.570	31–456	0.542–2.304	465
Cheng et al. [1983]	12.3	0.370–0.740	0.10–0.69	0.050–0.400	0.187–1.227	42–210	0.331–2.115	150
De Bortoli et al. [1958]*	4.57–7.77	0.229–0.589	6.90–13.8	0.651–6.726	0.052–0.768	0–874	1.609–5.805	54
Dell et al. [1969]	6.17	0.914–5.512	6.90	1.329–4.136	0.144–0.779	79–365	0.493–3.340	82
Era et al. [1967]	5.98	1.602–4.800	6.78–7.05	1.105–3.015	0.374–0.952	–1211–565	0.109–1.961	163
Griffel [1965]	6.22–37.5	0.610–1.972	3.45–10.3	0.637–18.58	–0.209–0.592	45–1209	1.401–8.107	402
Griffel [1965] SRL data	6.35–25.4	0.597–1.105	0.41–8.41	0.664–11.39	–0.253–0.484	66–1224	3.186–11.83	85
Groeneveld [1985]	10.0	1.000–2.000	7.90–20.0	0.282–2.805	–0.097–0.805	622–1733	1.133–5.479	118
Hassid et al. [1967]	2.49–2.51	1.590–2.391	2.94–6.09	0.369–3.858	–0.035–0.838	0–467	1.427–3.433	238
Hewitt et al. [1965]	9.30	0.229–3.048	0.10–0.21	0.091–0.301	0.161–1.083	–41–383	0.144–4.013	442
Jens and Lottes [1951]	5.74	0.625	3.45–13.8	1.302–10.60	–0.464—0.150	279–1310	2.965–11.92	48
Judd and Wilson [1967]	11.3	1.829	6.86–13.9	0.674–3.428	0.016–0.776	33–730	0.593–2.669	49
Kirillov et al. [1984]	7.71–8.09	0.990–6.000	6.37–18.1	0.494–4.154	–0.494–0.981	7–1537	0.110–7.700	2470
Landislau [1978]	4.00	0.200	0.42–1.00	0.884–5.504	–0.051—0.01	104–638	1.860–4.631	136
Lee and Obertelli [1963]*	5.59–11.5	0.216–2.007	4.14–11.0	0.678–4.421	0.000–0.910	9–690	1.104–8.107	295

TABLE 3.1. (CONT.)

References	Diameter (mm)	Length (m)	Pressure (MPa)	Mass Flux ($Mg.m^{-2}.s^{-1}$)	Dryout Quality (–)	Inlet Subcooling ($kJ.kg^{-1}$)	Critical Heat Flux ($MW.m^{-2}$)	No. of Data
Lee [1965]*	9.25–11.8	0.841–3.658	6.45–7.17	1.961–5.722	–0.002–0.462	12–584	1.000–4.306	274
Lee [1966]	14.1–44.7	0.635–1.524	8.24–12.6	0.332–3.410	–0.110–0.780	60–451	0.871–3.738	435
Leung et al. [1990]	5.45	2.511	5.03–9.71	1.168–9.938	0.210–0.578	6–316	0.656–3.058	66
Leung et al. [1990]	8.94	2.490	7.03–9.58	1.956–7.611	0.106–0.414	13–229	0.904–2.328	39
Lowdermilk et al. [1958]	4.00–4.80	0.119–0.991	0.10	0.027–4.866	0.030–1.236	317–331	0.167–9.525	113
Matzner [1963]*	12.8	1.930	6.86	0.933–1.978	0.075–0.592	54–947	1.686–3.372	25
Matzner et al. [1965]	10.2	2.438–4.877	6.89	1.193–9.560	0.008–0.693	48–1183	0.643–4.041	99
Mayinger [1967]	7.00	0.560–0.980	1.92–10.2	2.233–3.734	0.098–0.405	–239–314	0.924–5.618	128
Menegus [1959]***	3.6–92.4	-	0.19–6.80	0.006–13.70	–0.21–0.000	0–600	1.56–11.70	129
Nguyen and Yin [1975]	12.6	2.438–4.877	6.65–8.40	0.930–3.838	0.216–0.738	52–413	0.677–2.024	56
Rudzinski [1992]**	8.00	1.745	3.07–10.1	1.232–7.832	0.038–0.727	19–495	1.388–4.512	106
Smolin et al. [1962, 1964]	3.84–10.8	0.776–4.000	7.84–19.6	0.498–7.556	–0.132–0.795	5–1329	0.230–5.652	666
Smolin et al. [1979]	3.84–16.0	0.690–6.050	2.94–17.7	0.490–7.672	–0.136–0.789	4–1362	0.245–5.626	3009
Snoek [1988]	11.9	1.500	9.46–9.61	0.980–5.060	0.034–0.543	–481–356	0.423–3.037	33
Swenson [1962]*	10.5	1.753–1.803	13.8	0.678–1.763	0.178–0.502	41–565	0.587–1.063	25
Tapucu [1992]**	8.00	0.940–1.840	0.49–3.01	0.876–4.061	0.164–0.779	31–809	1.193–4.680	68
Thompson and Macbeth [1964]+	1.02–37.5	0.025–3.660	0.10–19.0	0.010–18.58	–0.820–1.577	0–1659	0.113–21.42	2356
Tong [1964]	6.22–12.9	0.380–3.660	5.17–13.8	0.678–14.00	0.002–0.502	5–1060	0.587–6.139	266
Yin et al. [1988]	13.4	3.658	1.03–21.2	1.938–2.081	0.075–0.431	0–493	0.583–1.864	287
Zenkevich et al. [1969]	3.99–15.1	0.250–6.000	5.88–19.6	0.498–9.876	–1.652–0.964	2–1644	0.136–14.76	5641
Zenkevich et al. [1971]	7.80–8.05	7.000–20.00	6.86–17.7	1.008–2.783	0.262–0.876	18–1549	0.470–1.283	392
Zenkevich [1974]++	4.80–12.6	1.000–6.000	5.89–19.6	0.497–6.694	–0.221–0.969	5–1381	0.230–4.740	840
Overall	0.62–92.4	0.011–20.00	0.10–21.2	0.006–24.27	–1.652–1.577	–1211–2711	0.109–44.71	28 017

* These data have already been included in Thompson and Macbeth's compilation.

** These data are used for validation only.

*** These data have not been used since the heated-length values of channels were not provided.

\+ Duplicated data of Becker (1963) have been removed.

++ Duplicated data of Zenkevich et al. (1969) have been removed.

3.3.2. Tube database

Table 3.1 lists a summary of data collected jointly by AECL and IPPE, and used in the development of the CHF prediction methods, including the CHF look up table [Groeneveld et al. (1996)]. Figure 3.2(a) shows that the conditions covered, although extensive, do leave open several gaps in the data. The non-proprietary part of the CHF databank, containing over 30 000 CHF data, obtained in directly heated tubes, has recently been deposited in the International Nuclear Safety Center Database at Argonne National Laboratory, described in Annex A.

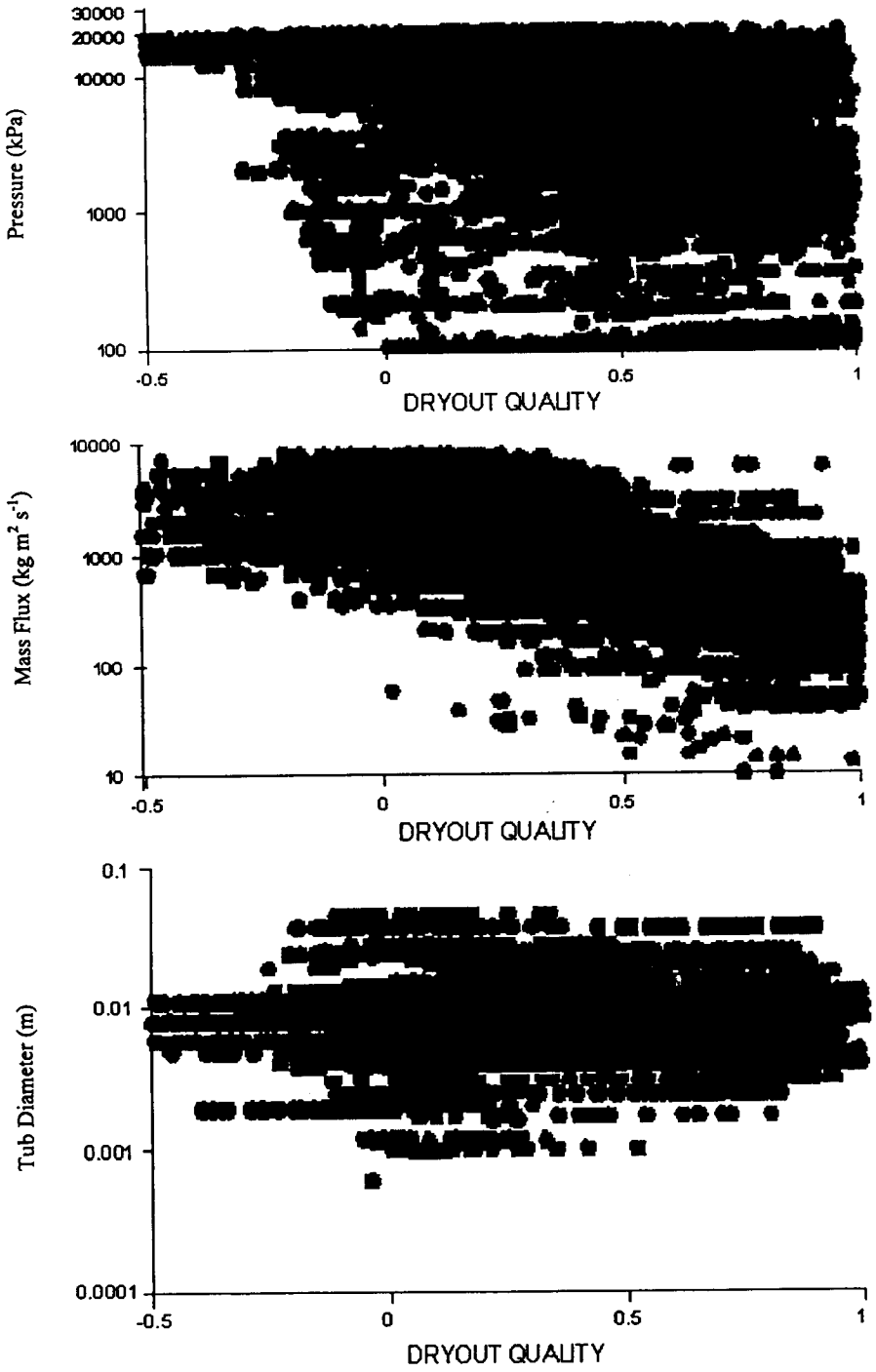

FIG. 3.2(a). Ranges of test conditions for the combined AECL-IPPE tube-CHF data bank.

The parameters controlling the CHF in tubes (for steady state conditions, and a uniform heat flux distributions) are:

(i) Primary: thermodynamic quality, mass velocity, pressure and diameter
(ii) Secondary: heated length, surface roughness, conductivity and tube wall thickness.

As the secondary parameters usually have a insignificant effect on CHF for conditions of interest, they may be ignored.

3.3.3. Bundle database

A large number of CHF experiments in bundles have been performed ranging from crude simulations of fuel bundles (e.g. annuli or 3-rod bundles) to full-scale simulations of actual fuel bundles. The following parameters have been found important in controlling CHF in fuel bundles:

(i) Flow parameters (pressure, mass flow, and quality). This includes cross section average flow conditions (this is usually reported) and distribution of flow parameters (i.e. distribution of enthalpy and flow across a bundle as evaluated by subchannel codes or other empirical means).
(ii) Bundle geometric parameters (number of rods, rod spacing, unheated flow boundary and heated length).
(iii) Rod bundle spacing devices and CHF enhancement devices (grids, appendages and mixing vanes) and their axial spacing.
(iv) Heat flux distribution (axial and radial heat flux distributions, and flux tilt across elements).

A number of surveys of bundle CHF data have been made. However because of the proprietary nature of bundle CHF data, these reviews are usually restricted as most bundle data (especially the recent ones) are unavailable or can only be obtained under special agreements. An earlier paper by Hughes (1974) provides a compilation of bundle CHF data sources. A more recent example of the ranges of conditions covered by specific bundle data sets is given in Figure 3.2(b) for the WWER bundle geometry [Macek (1998)], as can be seen the coverage is reasonably wide. However, as most bundle experiments still use fixed thermocouples, the reliability of the experimental CHF data as representing the initial occurrence of CHF may well be too optimistic (i.e. overpredicts the CHF). The more advanced sliding thermocouple technique (Schenk, 1990) has demonstrated that large differences (up to 20%) in bundle CHF can occur around the circumference of the most critical rod at the axial location corresponding to the initial CHF.

3.4. CHF PREDICTION METHODOLOGY

3.4.1. General

Because of the many possible fuel bundle geometric shapes, a wide range of possible flow conditions and the various flux distributions for AWCRs, it is impossible to predict the CHF for all cases with a single CHF prediction method and a reasonable degree of accuracy. The complexity of predicting the CHF in a nuclear fuel bundle may be best understood by first considering the prediction of CHF of a simplest experimental setup; a uniformly heated tube cooled internally by a fluid flowing at a steady rate vertically upwards. Here the CHF is a function of the following independent variables:

$$CHF = f(L_H, D_e, G, \Delta H_{in}, P, E) \tag{3.1}$$

where E takes into account the effect of the heated surface, i.e. surface roughness, thermal conductivity and wall thickness.

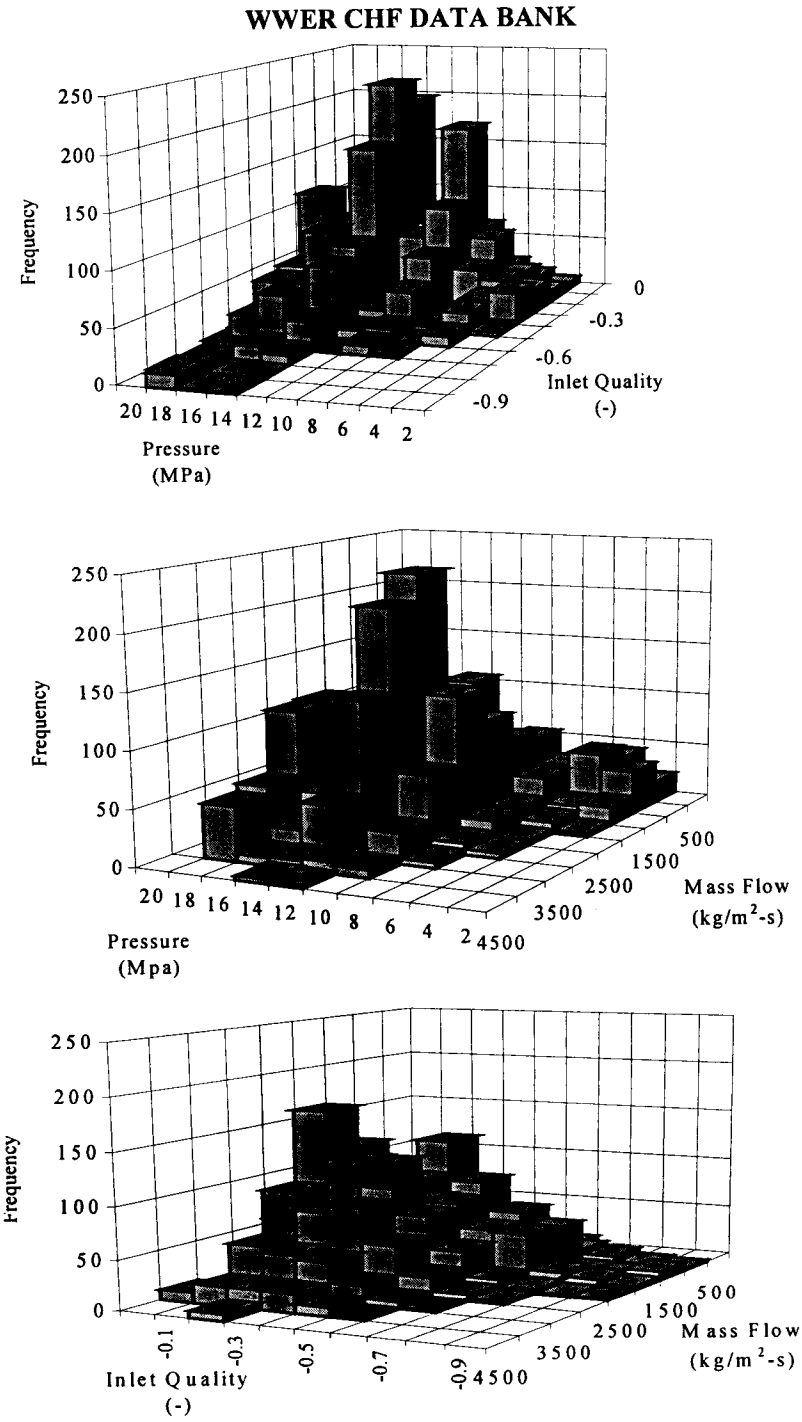

FIG. 3.2(b). Ranges of test conditions covered by the WWER CHF databank.

Despite the simplicity of the experimental setup, over 400 correlations for CHF in tubes are currently in existence. The present proliferation of correlations illustrates the complex state-of-the-art in predicting the CHF phenomenon even for a simple geometry at steady-state flow conditions. The complexity in predicting the CHF increases significantly for fuel bundle geometries during severe transients, when additional parameters characterizing the transient are required. This demonstrates the need to categorize the important CHF-controlling parameters and their ranges of interest. A methodology to categorize these parameters for thermalhydraulic parameters of interest has been proposed in Annex B.

In the following sections, analytical CHF prediction methods are discussed in Section 3.4.2, followed by empirical prediction methods in Section 3.4.3 which include empirical correlations as well as the CHF look up table. In Section 3.4.4 the application of CHF prediction methods to bundle geometries is described.

3.4.2. Analytical models

Analytical CHF models are based on the physical mechanisms and satisfy the conservation equations. They generally require a two-fluid model approach but occasionally must use a three-field approach (e.g. dispersed annular flow). Although the models have been improved significantly and usually predict the correct asymptotic trends, the evaluation process is complex and time-consuming. Furthermore, because of our limited understanding of the mechanisms involved, and the lack in measurements of interfacial parameters, the models are still less accurate than empirical correlations over the range of their database. An excellent review of the analytical CHF models has been presented by Weisman (1992). The most common CHF models that have met with some success are:

Annular film dryout model. This model is based on a mass balance on the liquid film in annular flow, and postulates that CHF corresponds to the depletion of the liquid film. Equations for droplet entrainment and deposition have been proposed. The model provides a reasonable predictions of CHF for the annular flow at medium to high pressures and flows and void fractions exceeding 50% [Hewitt and Hall-Taylor (1970)].

Bubbly layer model. This model postulates that CHF occurrence in the lower quality regime first occurs when the bubble layer covering the heated surface, becomes so thick and saturated with bubbles that liquid mixing between the heated surface and the cooler core liquid becomes insufficient. This model as proposed by Weisman and Pei (1983); and Ying and Weisman (1986) appear to predict the CHF with reasonable accuracy at high pressure, high flow and low quality conditions.

Helmholtz instability model. In pool boiling, the boiling crisis is reached when the flow of vapour leaving the heated surface is so large that it prevents a sufficient amount of liquid from reaching the surface to maintain the heated surface in the wet condition. The phenomenon that limits the inflow of liquid is the Helmholtz instability, which occurs when a counter-current flow of vapour and liquid becomes unstable. Zuber (1959) and Kutateladze (1952) have derived equations for the CHF based on the Helmholtz instability theory- their predictions agree with the CHF values measured in pool boiling systems. For very low flows, a modified version of this model as expressed by the Zuber-Griffith CHF correlation $\left(CHF_{PB}(1-\alpha)\right)$ appears reasonable for up- and down flow at flows less than 0.1 $Mg.m^{-2}.s^{-1}$ and $\alpha < 0.8$. However for $\alpha > 0.8$ this correlation significantly underpredicts the CHF. At these conditions the $1-\alpha$ correction is not recommended [Griffith et al. (1977)].

3.4.3. Empirical CHF prediction methods

Empirical CHF prediction methods may be subdivided into those based on inlet conditions and those based on local cross-sectional average (CSA) conditions.

3.4.3.1. Inlet-conditions-type prediction methods

These prediction methods are all in the form of empirical correlations, based on CSA inlet conditions (P, G, T_{in} or ΔH_{in}) and usually assume the "overall power" hypothesis. This hypothesis states that, for a given geometry and inlet conditions, the critical power N_{DO} (power corresponding to the first occurrence of CHF for that geometry) is independent of axial or radial heat flux distribution or

$$N_{DO} = f(P_{in}, G_{in}, T_{in}, c/s, L_H) \tag{3.2}$$

This will permit the use of CHF correlations derived from uniformly heated bundle data for the prediction of dryout power in non-uniformly heated bundles of identical geometry (i.e. identical cross section and heated length).

This technique is a reasonable one for obtaining a first estimate of dryout power; it gives reasonable estimate of dryout power in the annular flow regime for symmetric flux profiles and form factors ($=q_{max}/q_{avg}$) close to unity. However it is not recommended for form factors significantly different from unity.

This approach can also be used to predict the critical power of fuel channels with a fixed cross section, heated length, axial flux distribution (AFD) and radial flux distribution (RFD), irrespective of the form factor. If the experimental AFD and RFD represent the worst flux shapes from a CHF point of view, then the empirical correlations can be used for lower-bound predictions.

The Inlet-Conditions-Method cannot be used for predicting the location and magnitude of the CHF except when CHF initially occurs at the downstream end.

3.4.3.2. Local-conditions-type prediction methods

This type of prediction methods follow the local-conditions hypothesis which states that the local CHF is dependent only on the local conditions and not on upstream history. In principle, the local conditions hypothesis is sound if it is based on the true local conditions (which must include radial distribution of void, liquid and vapour velocity, liquid temperature and turbulent velocity fluctuation near the wall). Hence ideally

$$CHF = f(P, G, X_{DO}, c/s) \tag{3.3}$$

In practice only the local cross section average pressure, flow and quality are known and the assumption

$$CHF = f(\alpha(r), T_l(r), U_l(r), U_v(r), U_{l'}(r), \cdots, P, (c/s)) \tag{3.4}$$

that is often made. The local conditions approach, or variations thereof, is probably the most common method for predicting CHF. This form is more convenient than Eq. 3.1 since it depends on fewer parameters and permits the prediction of the location of CHF. One complication with this method is its ability (or lack of it) to account for the effect of AFD.

Two methods are frequently used to account for the effect of a non-uniform AFD on CHF: the boiling-length-average (BLA) approach, and the F-factor approach [Tong (1965, 1972), Kirillov and Yushenko (1996)]. The F-factor approach tends to modify CHF correlations designed for uniform heating, while in the boiling- length-average (or BLA) heat flux approach the heat flux distribution is modified. Lahey and Moody (1977) have shown that the two techniques are similar, yield similar answers and are reasonably successful in predicting the CHF for various non-uniform AFDs. Section 3.5.3.6 will describe the recommended approach for correcting for the effect of AFD.

Local conditions based empirical correlations. The large majority of the CHF prediction methods proposed are of this type. It is conservatively estimated that there are over 400 empirical correlations of this type proposed in the literature for directly heated tubes. Their main disadvantage is their limited range of application.

CHF table look up method. Since most empirical correlations and analytical models have a limited range of application, the need for a more general technique is obvious. As a basis of the generalized technique the local conditions hypothesis was used for the reasons given in Section 3.4.3.2 The initial attempt to construct a standard table of CHF values for a given geometry was made by Doroshchuk (1975), using a limited database of 5000 data. The CHF table approach, which is basically a normalized databank, has been continued at CENG-Grenoble, University of Ottawa, IPPE, and Chalk River using a much more extensive database (30 000 data). The recently completed International CHF table look up method [Groeneveld et al. (1996)] provides CHF values for water cooled tubes, at discrete values of pressure (P), mass flux (G), and quality (X), covering the ranges of 0.1–20 MPa, 0–7500 $kg.m^{-2}.s^{-1}$ (zero flow refers to pool-boiling conditions) and –50 to 100% vapour quality (negative qualities refer to subcooled conditions). Linear interpolation between table values is used for determining CHF. Extrapolation is usually not needed as the table covers a range of conditions much wider than any other prediction method. The CHF look up table and its derivation are presented in Appendix II.

Compared to other available prediction methods, the tabular approach has the following advantages: (i) greater accuracy, (ii) wider range of application, (iii) correct asymptotic trend (iv) requires less computing time and (v) can be easily updated if additional data become available. Although tabular techniques were initially developed for tubular geometries, and have been successfully used in subchannel codes, their greatest potential for application is in predicting the consequences of postulated Loss of coolant-Accidents (LOCA). To apply the tables to transient heat transfer in bundles requires the use of adjustment factors to correct for geometry, flux shape, and possibly transient effects. Here the advantages of the tabular technique (wide range of application, greater accuracy and more efficient in computing) are particularly important to the user.

Although promising, the look up table approach has certain disadvantages such as (i) it is a purely empirical prediction method and hence it does not reflect any of the physics, and (ii) could introduce erroneous trends if the underlying database is subject to experimental errors. Despite these reservations, the look up table approach is currently considered to be more accurate than other prediction methods for the CHF for most situations of interest.

3.4.4. Application to bundle geometries

Prediction of the critical power in untested fuel bundle geometries remains unreliable. Effects of flux distribution, grid spacers and bundle array dimensions are not well understood. The

next two approaches are commonly used, while the third one has more recently been proposed and an alternative.

(1) *Empirical approach*: The empirical CHF predictions methods use cross-sectional average conditions to predict the CHF or critical power and are designed for tubes or bundles. For bundles for which experimental data can be obtained (using an electrically heated fuel bundle simulator, having a fixed axial and radial flux distribution) a variant of the following methodology is frequently employed:

- obtain sufficient data for deriving an empirical CHF correlation for conditions of primary interest;
- extrapolate the empirical correlations (which are usually based on a given axial and radial flux distribution) to other flux distributions of interest using the change in CHF as predicted by (i) subchannel codes (see below) or (ii) empirical methods to account for changes in the upstream flux shape (as described in the previous section;
- similarly extrapolate to other conditions not tested in the full scale simulation tests using trends observed in simpler geometries, or as predicted by subchannel codes.

(2) *Subchannel approach:* The subchannel approach is basically different from the empirical approach as it predicts the axial variation in flow and enthalpy for each subchannel. It is particularly useful for bundles for which no direct experimental data are available. The following methodology is normally followed for bundle CHF prediction based on the subchannel analysis approach:

- employ subchannel codes to predict the flow and enthalpy predictions across the bundle
- employ subchannel CHF models (basically modified tube CHF prediction methods) for predicting the initial CHF occurrence anywhere in the bundle.

Two definitions of subchannels are currently in use. The conventional approach defines subchannel boundaries by lines between rod centre and is used in subchannel codes such as ASSERT [Carver et al. (1993)], COBRA [Owen 1971)]; ANTEO [Cervolani (1995)] or HAMBO [Bowring (1967)]. The rod centered approach defines subchannel boundaries by lines of zero stress between rods and is used primarily to predict CHF in the annular flow regime [using Hewitt and Hall-Taylor's (1970)] annular flow model or an equivalent CHF correlation. A thorough review of subchannel prediction methods is presented by Weisman (1975).

(3) *Enthalpy imbalance approach.* An alternative to the subchannel approach has been described by McPherson (1971) (applied to various bundle geometries contained in pressure tubes), Bobkov (1995, 1997) (applied to excentric annuli and bundle subchannels), and Leung (1997) (applied to 37 element bundle CHF predictions). This approach, which was recently reviewed by Kirillov et al. (1996b), considers the differences in enthalpy rise rates among bundle subchannels, and based on this defines a quality imbalance, ΔX for that bundle. This quality imbalance (a variation of this is the enthalpy imbalance number specified by McPherson(1971)) represents the difference in qualities between the cross section average bundle quality and the maximum bundle subchannel quality for a given cross-section. The difficulty is in predicting the ΔX value; no general expression for the enthalpy imbalance is yet available but ad hoc expressions for specific bundle geometries have been proposed. In general,

$\Delta H = f(\delta / d, \Delta X_{max})$ where δ / d is the element gap/diameter ratio, and ΔX_{max} is the maximum quality imbalance, which depends on the difference between the subchannel enthalpy of the critical subchannel for zero cross flow and the cross-sectional average enthalpy. Once a general expression for ΔX is found (this may well require a fit of a randomly-generated database using a subchannel code) the bundle CHF can be obtained from the tube CHF look up table [Groeneveld et al. (1996)] for the critical subchannel. In equation form this bundle CHF methodology is as follows:

$$CHF_{bundle}(P,G,X) = CHF_{tube}(P,G,Xo).K_1.K_3.K_4.K_5. \quad (3.5)$$

where:

$X_0 = X + \Delta X$ and K_1, K_3, etc. are correction factors described in Section 3.5.3. The impact of flow imbalance on CHF is usually assumed to be negligible or assumed to be incorporated in ΔX.

3.5. RECOMMENDED CHF PREDICTION METHOD FOR ADVANCED WATER COOLED REACTORS

To provide precise predictions of CHF for advanced water cooled reactors fuel bundles is a nearly impossible task as advanced water cooled reactors designs include a variety of bundle cross sections as well as element spacer designs. This section therefore will recommend a generic approach of predicting CHF in untested bundle geometries. The basis of almost any generic bundle prediction method is a tube CHF prediction method, because (i) the parametric trends with P, G, and X are similar in tubes and in bundles, and (ii) tube CHF prediction methods are generally used in subchannel codes to predict the CHF in bundles.

In this section we will first discuss the recommended tube CHF prediction method and will subsequently describe how this method can be used for predicting the CHF in bundle geometries.

3.5.1. Tubes

The recommended CHF prediction is the recently published CHF look up table for tube [Groeneveld et al. (1996)] which was based on cooperation of several international groups, notably AECL in Canada and IPPE in Russia. This CHF prediction method is a slight modification from previous tables [Groeneveld et al. (1993)], has been validated independently by others as described in Section 3.6.1 and has resulted into better CHF predictions compared to other existing CHF correlations, both in accuracy and range of validity. Groeneveld et al. (1996) have presented a complete description of the new table including its derivation, and accuracy with respect to the world database, and a comparison with other widely used CHF prediction methods.

3.5.2. Rod bundles

The tube CHF look up [Groeneveld et al. (1996), see also Appendix II] needs to be converted into a prediction method for bundle geometries. To do this, two approaches may be used:

(1) Subchannel based approach, as described in Section 3.4.4 item 2, and
(2) Cross-sectional average bundle approach as described in Section 3.4.4 item 3.

Ideally a subchannel code should be used to predict the CHF for bundle geometry. Several subchannel codes are currently in existence [see review article by Weisman (1975) for more details] but their validation tends to be limited to a narrow range of bundle geometries and flow conditions for which their constitutive relations have been tuned to agree with the experimental database. With time this limitation is expected to be resolved as more appropriate constitutive relations are being derived and the robustness of the codes is continuously being improved.

In both of the above approaches the CHF needs to be modified to account for bundle specific or subchannel specific effects. The following correction factor methodology is adopted to evaluate the bundle or subchannel CHF:

$$CHF_{bundle} = CHF_{table} \times K_1 \times K_2 \times K_3 \times K_4 \times K_5 \times K_6 \times K_7 \times K_8 \tag{3.6}$$

where

CHF_{bundle} is cross section average value of the heat flux at which the CHF first occurs at the cross-section, CHF_{table} is the CHF value for a tube as found in the look up table for the same cross-sectional average values of P and G, and K_1 to K_8 are correction factors to account for specific bundle effects. Note that the form of this equation implies that all correction factors are independent. Many factors are somewhat interdependent, but these interdependencies are assumed to be second order effects unless indicated otherwise in the following sections. The correction factors are described in Section 3.5.3.

3.5.3. Correction factors

Table 3.2 lists the most common bundle specific or subchannel specific effects which are expected to affect the CHF. As these effects are not reflected by the database for the tube look up table, correction factors have been derived. Table 3.3 lists approximate relationships for the correction factors. The sections below elaborate on the more important correction factors.

3.5.3.1. Diameter

Experiments in tubes have shown a strong effect of tube diameter on CHF. A number of investigators have discussed this effect. Recently Wong (1996) has made a thorough systematic study of this effect and concluded that the original approach using the equation:

$$K_1 = \frac{CHF_D}{CHF_{D=8mm}} = \left(\frac{D}{8}\right)^n \quad (3.7)$$

where

n is between –1/3 and –1/2 and appears to be valid for the majority of the data. Slight improvements could be made by assuming n = f (P, G, X) but the improvements were minor and limited to the range of experimental data on which the new n-function was based. Cheng and Erbacher (1997) have recently performed additional experiments in Freon and noticed that the change in CHF with diameter according to Eq. 3.7 appears to valid (with n ~ –1/2) for diameters equal or smaller than 8 mm but no effect of diameter (or a very small effect) on CHF was observed for diameters greater than 8 mm. Note that Cheng's data were obtained primarily at subcooled or low quality conditions. Kirillov and Yushenka (1996) also noted disagreements in the diameter effect on CHF for negative qualities but the general agreement for D 8mm with n between –1/3 and –1/2. Despite this disagreement, the recommendation by Groeneveld (1996) using n = –1/2 , and subsequently confirmed by Wong (1996), appears to be a simple compromise which agrees reasonably with the bulk of the available data.

Although K_1 was derived empirically from tube data, the diameter correction factor has been applied directly to subchannels as well where the D_{hy} is used. Because of lack of data on CHF in various sizes of subchannels, the validity of the approach as applied to subchannels has not been confirmed.

TABLE 3.2. CHF SEPARATE EFFECTS ENCOUNTERED IN FUEL BUNDLES

GENERAL	DETAILS OF SEPARATE EFFECTS
Global Flow Area Effects:	- n-rod bundle where n>>3 and all subchannels identical except corners or cold-wall-adjacent subchannels (e.g., square or triangular arrays of subchannels) - n-rods where n>>3 and adjacent subchannels are generally not equal (e.g. 37-rod bundle geometries inside round tubes)
Subchannel Effects	- Subchannel size/shape (similarity to tube) - Cold wall effect - Distorted subchannels (due to bowing, clad strain, pressure tube creep) - Misaligned bundles (CANDU case)
Length Effects	Similar to appendage effects
Spacers/Bundle Appendages Effects	- mixing grids - attached spacers/ bearing pads/ endplates (CANDU)
Flow Orientation Effects	- Vertically upward - Vertically downward - Horizontal
Axial/Radial Flux Distribution Effects	- Axial flux distribution (flux peaking/global flux distribution) - Radial Flux Distribution (global RFD effect, cold wall effect, flux tilt across an element)
Flow Parameter Effects	- mass flow (incl. zero flow or pool boiling / flow stagnation case)
Transient Effects	- Power/Flow/Pressure transients - Combined transients
Effect of Fluid Type	- Light water - Heavy water - Modelling fluids (Freons) in conjunction with a CHF Fluid-to-fluid modelling technique

TABLE 3.3. SUMMARY OF CORRECTION FACTORS APPLICABLE TO THE CHF LOOK-UP TABLE

FACTOR	FORM	COMMENTS
K_1, Subchannel or Tube-Diameter Cross-Section Geometry Factor	For $2 \le D_{hy} \le 25$ mm: $K_1 = (0.008/D_{hy})^{1/2}$ For $D_{hy} > 25$ mm: $K_1 = 0.57$	Includes the observed diameter effect on CHF. This effect is slightly quality dependent.
K_2, Bundle-Geometry Factor	$K_2 = \min[1,(0.5+2\,\delta/d)\exp(-0.5\,x^{1/3}]$	This is a tentative expression, an empirically derived factor is preferred. K_2 is also a weak function of P, G and X.
K_3, Mid-Plane Spacer Factor for a 37-element Bundle	$K_3 = 1 + A\exp(-B\,L_{sp}/D_{hy})$ $A = 1.5\,K_L^{0.5}(G/1000)^{0.2}$ $B = 0.10$	This factor has been validated over a limited range of spacer geometries.
K_4, Heated-Length Factor	For $L/D_{hy} \ge 5$: $K_4 = \exp[(D_{hy}/L)\exp(2\alpha_h)]$ $\alpha_h = X\rho_f/[X\rho_f + (1-X)\rho_g]$	Inclusion of α_h correctly predicts the diminishing length effect at subcooled conditions.
K_5, Axial Flux Distribution Factor	For $X \le 0$: $K_5 = 1.0$ For $X > 0$: $K_5 = q_{loc}/q_{BLA}$	Tong's F-factor method (1972) may also be used within narrow ranges of conditions.
K_6, Radial or Circumferential Flux Distribution Factor	For $X > 0$: $K_6 = q(z)_{avg}/q(z)_{max}$ For $X \le 0$: $K_6 = 1.0$	Tentative recommendation only and to be used with well-balanced bundle. May be used for estimating the effect of flux tilts across elements. Otherwise method of Yin (1991) is recommended.
K_7, Flow-Orientation Factor	$K_7 = 1-\exp(-(T_1/3)^{0.5})$ where $T_1 = \left(\frac{1-X}{1-\alpha}\right)^2 \frac{f_L G^2}{g\,D_{hy}\,\rho_f(\rho_f-\rho_g)\alpha^{0.5}}$ f_L is the friction factor of the channel	This equation was developed by Wong and Groeneveld (1990) based on a balance of turbulent and gravitational forces. The void fraction is evaluated with the correlation of Premoli et al. (1970).
K_8, Vertical Low-Flow Factor	G<-400 kg.m^{-2}.s^{-1} or X<<0: $K_8 = 1$ -400 <G < 0 kg.m^{-2}.s^{-1}: Use linear interpolation between table value for upward flow and value predicted from $CHF = CHF_{G=0,X=0}(1-\alpha_{hom})C_1$	For $\alpha_h < 0.8$: $C_1 = 1.0$ For $\alpha_{hom} \ge 0.8$: $C_1 = \frac{0.8 + 0.2\,\rho_f/\rho_g}{\alpha_{hom} + (1-\alpha_{hom})\,\rho_f/\rho_g}$ Minus sign refers to downward flow. G=0, X=0 refers to pool boiling.

3.5.3.2. Bundle

Prediction of the critical power in untested fuel bundle geometries such as many of the proposed advanced water cooled reactor fuel bundles has a higher uncertainty especially if the flux distribution, grid spacer shape and bundle array dimensions are different from those tested previously. The most reliable approach aside from ad hoc testing, is to employ a subchannel analysis as described in Section 3.4.5 (at a limited range of conditions of interest) to valuate the bundle CHF analytically, and to derive a bundle correction factor expressed as

$K_2 = CHF_{bundle}/CHF_{table}$ for use inside a systems code. In the absence of any test data Eq. 3.8 is the simplest one available and follows the correct asymptotic trends.

$$K_2 = \text{Min}[1.0,(0.5 + 2\delta/d)\exp(-0.5\,x^{1/3})] \tag{3.8}$$

Note that further work in this area is required and that the approach based on the enthalpy imbalance as embodied in Equation 3.5 [Kirillov (1996b)] is the most promising

$$K_2 = \frac{CHF_{tube\text{-}table}(P,G,X+\Delta X)}{CHF_{tube\text{-}table}(P,G,X)} \tag{3.9}$$

one. This would then simply change the bundle correction factor to the form of Equation 3.9, but requires an empirical expression for ΔX (see also Section 3.4.4 item 3 and the references of Appendix III for further details).

3.5.3.3. Spacer

A number of researchers have investigated the effect of spacing devices on CHF or critical power. Figure 3.3 shows the various types of spacers used in these studies. In general a significant increase in local CHF was observed just downstream of the spacers. This increase usually decays slowly with distance downstream as illustrated in Fig. 3.4. The increase is primarily due to the higher turbulence level of the two-phase flow, which can strongly suppress the occurrence of CHF and the improved intersubchannel mixing. In experiments on CANDU fuel bundles, this increase in CHF is most pronounced just downstream of spacer planes and bundle junctions, where increases in local CHF of over 150% have been observed.

The strong CHF-enhancement effect has been confirmed by others, e.g. Tong (1972). It has been expressed by the enhancement factor:

$$K_3 = 1 + A\exp\left(-B\frac{L_{sp}}{D_{hy}}\right) \tag{3.10}$$

where

$A = 1.5\ K^{0.5}\ (0.001G)^{0.2}$ (K is the pressure loss coefficient of the spacing device) and $B = 0.1$ were proposed by Groeneveld (1989).

Subsequent studies at CRL and IPPE have noted that using the pressure loss coefficient itself may not be sufficient because of the apparent insensitivity of the CHF enhancement to streamlining of the grid spacer, and an expression using the flow blockage area may be more appropriate [Kirillov (1997)]. Note that these values will still be approximations as the shape of the spacer and the element gap are also important parameters.

In bundles the length factor is no longer needed as this effect is already incorporated in the spacer correction factor (hence $K_4 = 1$).

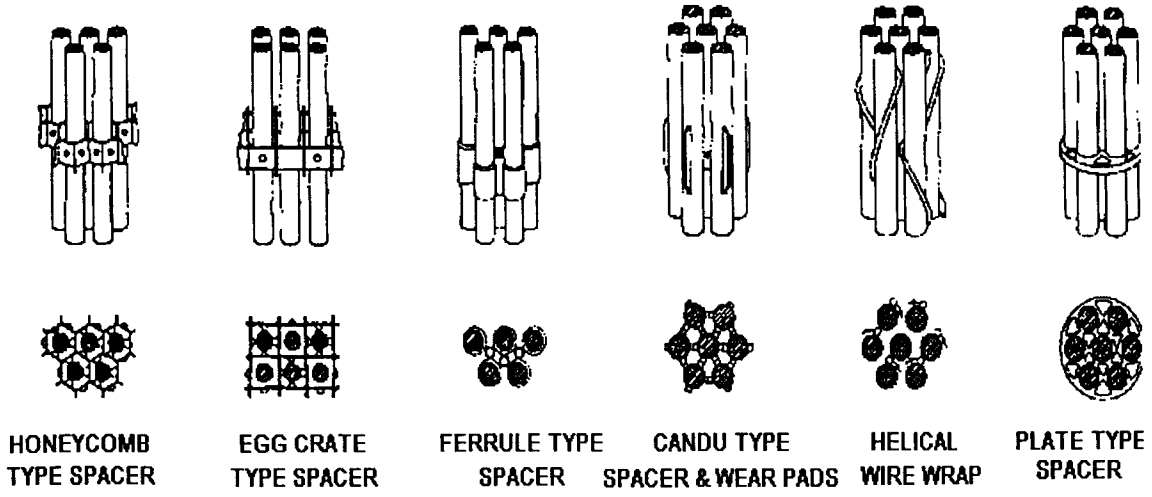

FIG. 3.3. Different types of rod spacing devices.

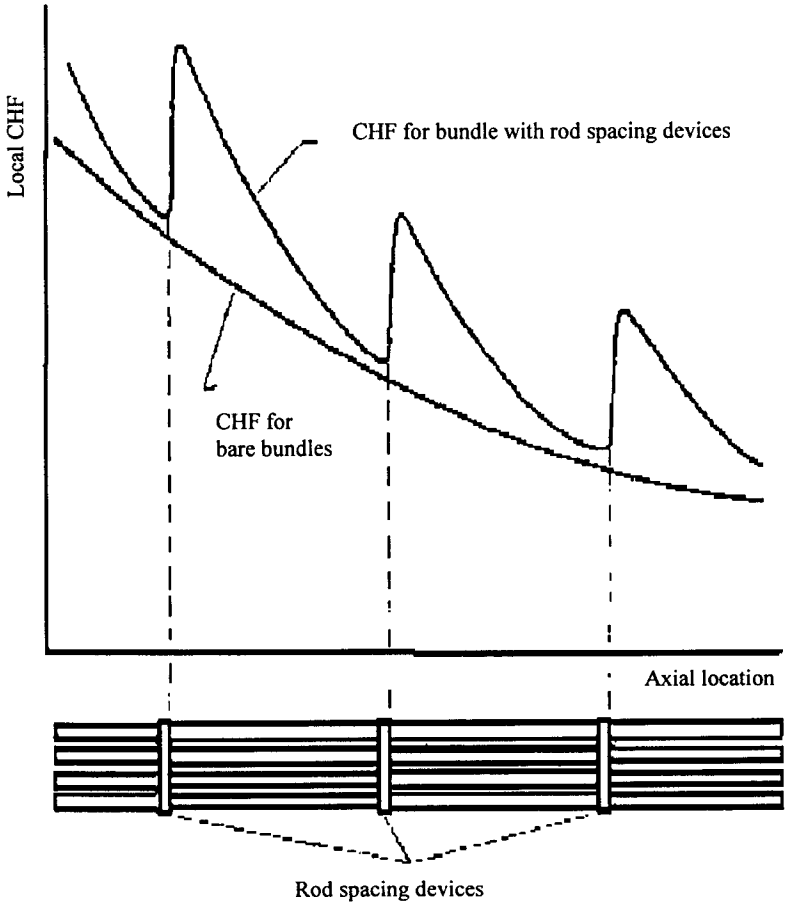

FIG. 3.4. Exponential decaying CHF enhancement downstream of a spacing device.

3.5.3.4. Axial flux distribution

Many experimenters have studied the effect of axial flux distribution (AFD) on critical power [e.g. Collier (1981); Tong (1972); Todreas and Rohsenow (1965); Groeneveld (1975), Kirillov (1997)]. The common observation in all these studies is that the AFD has a strong effect on the CHF in the annular flow regime but this effect tends to disappear altogether for the DNB-type of CHF. The effect of AFD on CHF can be accounted for by using the boiling-length-average (BLA) heat flux instead of the local heat flux. The BLA heat flux is defined as:

$$q_{BLA} = \frac{1}{L_B} \int_{L_{x=0}}^{L_{x=x_{DO}}} \phi dL \tag{3.11}$$

$$L_B = \frac{G H_{fg} D_{he}}{4 X_{DO} q_{BLA}} \tag{3.12}$$

where the BLA heat flux has been incorporated in the AFD correction factor K_5 defined as:

$K_5 = \rho_{local} / \rho_{BLA}$ for $X > 0.0$

$K_5 = 1.0$ for $X \leq 0.0$

3.5.3.5. Radial flux distribution

The ideal tool for evaluating the RFD effect on dryout power or CHF is a reliable subchannel code. Subchannel codes can also consider the effect of flux tilt across elements by accounting for the different heat flux values around the circumference of a fuel pin. However subchannel codes are complex, expensive to run and have usually a limited range validity. Hence a more empirical approach is often preferred. The RFD correction factor falls between two extreme values: (i) for open bundles where the subchannel flow and enthalpy imbalance is small, and the maximum heat flux controls the initial occurrence of CHF. For such a case K_2 is close to unity (or ΔX is close to zero) and K_6 is approximately equal to $q_{avg}(z)/q_{max}(z)$, where q_{max} represents the maximum heat flux for the subchannel and q_{avg} is the cross section average heat flux, and (ii) for very tight bundles ($\delta/D \leq 0.1$) where the communication between subchannels is severely hampered and K_6 (if used in conjunction with K_2 as expressed by Equation 3.8) depends also on the subchannel and flow imbalance. For this case a technique for obtaining a K_6 value based on RFD was proposed by Yin et al. (1991), but this still requires knowledge of the RFD corresponding to simultaneous CHF occurrence across the bundle (this could possibly be obtained from subchannel codes). However if the K_2 value is obtained from Equation 3.9 (based on ΔX), no further correction for K_6 beyond the q_{avg}/q_{max} value is required.

3.5.3.6. Flow orientation

The effect of orientation is important for CANDU reactors, where the fuel channels are oriented horizontally, and for conventional boilers, where many of the boiler tubes are inclined. The approach taken is to correct the vertical flow CHF by a penalty factor to account for the deleterious effects of flow stratification. For fully stratified flow, the CHF = 0 (i.e. $K_7 = 0$), while for a flow regime unaffected by flow stratification, $CHF_{ver} = CHF_{hor}$ or $K_7 = 1.0$. Using a mechanistically based flow regime map [e.g. Taitel and Dukler (1975)]

permits the determination of the mass flux threshold G_1, corresponding to the onset of complete flow stratification (where liquid no longer touches the top of the channel, i.e. the CHF = 0) and the mass flux threshold G_2, corresponding to the first noticeable effect of stratification on the phase distribution. Table 3.3 shows a simple expression for the correction factor K_7 having the correct asymptotic trends. A more rigorous expression for the flow stratification correction factor was derived by Wong et al. (1990), based on both the flow regime and a force balance on the phases. Their expression for the correction factor K_7 resulted in accurate predictions of the CHF in horizontal flow in various fluids over a wide range of conditions.

3.6. ASSESSMENT OF ACCURACY OF THE RECOMMENDED PREDICTION METHODS

3.6.1. CHF look up table assessment

The CHF look up table described in Section 3.5.1 and presented in Appendix II as well as earlier versions of the look up table have been assessed extensively. The most recent assessment was made at KAIST, Korea, by Baek et al. (1996) using their database. Their assessment confirms the error statistics reported by Groeneveld et al. (1996), and confirms the improved prediction capability compared with the 1986 AECL-University of Ontario (UO) Look-up Table [Groeneveld et al. (1986)]. In addition the distribution of CHF data and the error distribution of the CHF look up table as a function of pressure, flow and quality intervals are given in Table 3.4.

Earlier assessments by Smith (1986) and Weaver (1995) indicated the suitability of the table look up approach and has resulted in its use in systems codes such as CATHARE [Bestion (1990)], THERMOHYDRAULIK [Ulrych (1993)], ASSERT [Kiteley (1991), Carver (1993)] and RELAP [Weaver (1995)]. Assessments were also made by Aksan et al.(1995) and Faluomi and Aksan (1997) where an earlier version of the look up table (CHF-UO table) was compared to other leading CHF correlations and the impact of the differences in CHF predictions on nuclear plant transients of interest was assessed.

3.6.2. Accuracy of bundle CHF prediction methods

As indicated in the previous sections, the prediction of bundle CHF is much more difficult than the tube-based predictions. In addition the database has a much greater uncertainty because of the relatively crude fixed thermocouple technique for detecting initial CHF occurrence. Prediction accuracy for a well tested bundle geometry is usually quite reasonable (frequently within 5% at a 2σ confidence level for a given inlet conditions) but this is due to the fine-tuning of the correlation/subchannel code with empirically derived coefficients. For new AWCR geometries the accuracy is significantly reduced and could well be greater than 10% at 2σ.

An independent assessment was made by Chun et al. (1997) of the CHF look up table as a prediction method for bundles in conjunction with a subchannel code (COBRA-IV-1). They compared the look up table with six leading CHF prediction methods [Biasi et al. (1967)]; W-3, EPRI-1 as referred to by Chun et al. (1997); Katto and Ohno (1984); and two CHF models [Weisman and Ying (1985); Lin et al. (1989)]. They concluded that, for AWCR design applications, in the absence of a database, the look up table has the greatest potential as a general predictor for CHF in rod bundles. The CHF look up table has also been used and assessed in conjunction with the ASSERT subchannel code [Carver (1993,1995)] and the ANTEO subchannel code [Cervolani (1995)].

For specific bundle geometries a bundle specific look up table can be used. Good success has been reported with the recent IPPE bundle CHF look up table for WWER geometries. This table is reproduced in Appendix III where a brief description of its potential use is also provided.

TABLE 3.4. ERROR-DISTRIBUTION TABLE FOR LOCALIZED RANGES OF FLOW CONDITIONS

Pressure Range (kPa)		100 to 1000				1000 to 5000				5000 to 8000			
Mass Flux Range ($kg.m^{-2}.s^{-1}$)		Quality Range				Quality Range				Quality Range			
		-0.5--0.1	-0.1-0.2	0.2-0.5	0.5-1	-0.5--0.1	-0.1-0.2	0.2-0.5	0.5-1	-0.5--0.1	-0.1-0.2	0.2-0.5	0.5-1
0 to 1000	No. of Data	0	1	55	523	0	0	87	1755	0	1	141	776
	Avg. Error (%)	0	31.9	4.7	0.4	0	0	-8.1	-3.5	0	4.6	-1.0	-1.4
	Rms Error (%)	0	31.9	16.7	8.8	0	0	10.2	7.2	0	4.6	5.4	5.9
	No. of Data Set	0	1	4	5	0	0	7	8	0	1	12	15
1000 to 3000	No. of Data	0	0	115	21	0	45	766	416	2	454	1340	747
	Avg. Error (%)	0	0	12.3	2.1	0	-2.5	-2.7	-1.9	-4.2	0.0	0.7	0.0
	Rms Error (%)	0	0	25.7	18.5	0	4.1	10.2	10.8	4.2	10.4	4.4	8.2
	No. of Data Set	0	0	6	4	0	5	10	8	2	17	22	15
3000 to 4500	No. of Data	0	1	33	0	1	67	248	0	0	486	493	0
	Avg. Error (%)	0	14.3	9.9	0	13.3	1.2	4.8	0	0	1.9	0.3	0
	Rms Error (%)	0	14.3	20.1	0	13.3	12.7	12.0	0	0	9.9	3.8	0
	No. of Data Set	0	1	2	0	1	7	7	0	0	18	19	0
4500 to 6000	No. of Data	0	0	0	0	0	34	28	0	6	228	126	0
	Avg. Error (%)	0	0	0	0	0	4.9	5.7	0	3.0	1.0	2.1	0
	Rms Error (%)	0	0	0	0	0	10.3	11.9	0	8.3	5.3	5.6	0
	No. of Data Set	0	0	0	0	0	7	5	0	3	13	9	0
6000 to 8000	No. of Data	0	0	0	0	0	19	22	0	0	95	15	0
	Avg. Error (%)	0	0	0	0	0	24.9	11.9	0	0	7.2	9.6	0
	Rms Error (%)	0	0	0	0	0	61.9	17.3	0	0	11.0	12.3	0
	No. of Data Set	0	0	0	0	0	3	2	0	0	9	5	0

Pressure Range (kPa)		8000 to 12 000				12 000 to 16 000				16 000 to 20 000			
0 to 1000	No. of Data	0	27	249	535	0	178	621	388	32	154	333	215
	Avg. Error (%)	0	1.3	1.8	-0.6	0	-0.6	1.2	0.7	1.5	-0.3	0.2	0.7
	Rms Error (%)	0	5.0	11.9	8.4	0	6.1	6.1	10.4	4.8	4.4	5.0	8.9
	No. of Data Set	0	5	12	13	0	7	13	10	3	8	9	8
1000 to 3000	No. of Data	3	671	1457	216	86	1234	1763	15	135	570	1031	16
	Avg. Error (%)	3.8	0.4	2.5	3.1	-0.4	1.2	1.8	-4.2	1.1	0.7	-0.5	0.3
	Rms Error (%)	4.7	4.8	9.1	10.7	5.2	4.7	6.0	5.3	5.5	4.1	4.8	3.8
	No. of Data Set	3	18	23	12	8	15	13	4	8	9	9	3
3000 to 4500	No. of Data	3	538	392	0	25	513	337	0	59	255	272	3
	Avg. Error (%)	3.2	1.4	0.2	0	2.2	2.5	-0.4	0	2.3	4.6	1.3	-6.7
	Rms Error (%)	3.7	4.7	6.2	0	5.6	5.7	5.2	0	6.4	8.6	5.7	10.6
	No. of Data Set	2	18	12	0	3	10	8	0	5	9	8	2
4500 to 6000	No. of Data	0	272	193	0	28	221	124	0	14	134	106	0
	Avg. Error (%)	0	0.9	0.9	0	4.0	4.1	3.5	0	0.9	6.6	2.6	0
	Rms Error (%)	0	5.6	7.8	0	5.4	6.9	6.4	0	1.6	9.3	5.9	0
	No. of Data Set	0	12	10	0	3	9	7	0	3	7	7	0
6000 to 8000	No. of Data	0	143	124	0	0	47	18	0	6	34	9	0
	Avg. Error (%)	0	4.9	3.6	0	0	6.2	-1.8	0	-1.5	7.5	-2.7	0
	Rms Error (%)	0	13.6	8.3	0	0	14.9	3.6	0	1.9	12.1	6.0	0
	No. of Data Set	0	11	7	0	0	6	3	0	2	6	5	0

3.6.3. Impact of accuracy of CHF model on cladding temperature prediction

CHF prediction methods are usually integrated in reactor safety codes and are used to predict the cladding temperature. This brings up the concern whether the same CHF prediction method is used for maximum cladding temperature prediction and for predicting the hydraulics response in a channel (see Section 3.7.1 for more details). Various investigators have considered the sensitivity of the CHF model in their codes on the cladding temperature transient. Belsito and D'Auria (1995) used an earlier version of the CHF look up table [Groeneveld et al. (1986)] and concluded that the discrepancies between pre-test and post-test analysis is due to the uncertainty in the boundary conditions and the calculation of the pressure at CHF.

post-dryout heat transfer

3.7. CHF CONCERNING ACCIDENT CONDITIONS

3.7.1. General

In the previous discussion of CHF prediction methods it was assumed that the prediction of the initial occurrence of CHF is of paramount importance (as it is for setting the operating power for a reactor). However to predict the proper thermalhydraulic/neutronic response (they are linked) to a more massive occurrence of CHF across the core, knowledge of how CHF occurrence spreads across the reactor core is required. This will permit an evaluation of how much of the heat generated by the fuel is used for evaporation (usually 100% for saturated boiling if the CHF has not been exceeded), and how much is used for heating up the fuel (this could be close to 100% during fast transients where the fuel cladding has just experienced CHF and is heating up to the corresponding film boiling temperature). Systems codes ideally should be based on this more detailed (3-D) approach of evaluating the spread of CHF occurrence (or drypatch size) across the core.

The drypatch size predictions depends directly on the choice of the time steps, axial node size and size of nodes across the core. Detailed experiments on 37-rod fuel bundle simulators using sliding thermocouples [Schenk et al. (1990)] have clearly indicated that it requires a significant rise in power (10–25%) just to spread the CHF around one element, while the same measurements indicated that fuel element supports (spacers, endplates, grids) usually have a large local impact (~100–200%) on CHF (e.g. see Section 3.5.3).

A number of papers have been published where an assessment was made of the implementation impact of the CHF look up table [Faluomi and Aksan (1997); Aksan et al. (1995); Weaver (1991)]. They generally confirm the difficulty of individual CHF correlations in following the complex CHF variations with flow conditions.

3.7.2. Effect of the axial/radial node size

It is now known that CHF is strongly affected by fuel element supports such as grid spacers (which frequently are equipped with mixing vanes), and spacers/endplates in CANDU reactors. Increases in CHF of over 100% (for the same local flow conditions) due solely to the presence of an upstream fuel rod support have been measured. This increase in CHF decreases exponentially with distance downstream from the rod spacer as shown by Equation 3.10. The net impact of this depends on the specifics of the bundle geometry and rod support type: decreases in CHF by up to 50% over a distance of 12 cm have been measured [Doerffer

(1996)]. It is recommended to use as small an axial node length as practically possible (less than 5 cm) for those types of safety analysis where the size of the drypatch is important.

CHF does not occur simultaneously across a bundle, and in fact even across a 37 element bundle, it requires typically 50% increase power (for the same local flow conditions P, G and X) to have the CHF spread across the half the bundle geometry, and over 100% to spread across the whole geometry. Figures 3.5 and 3.6 [D'Auria (1997)] also illustrate the non-uniformity in CHF occurrence as measured in the LOBI and BETHSY test facilities [Faluomi and Aksan (1997)]; for square array bundle geometries. This limits the use of a 1-D system code in representing the CHF behaviour and its impact on void generation and neutron flux behaviour for PHWR.

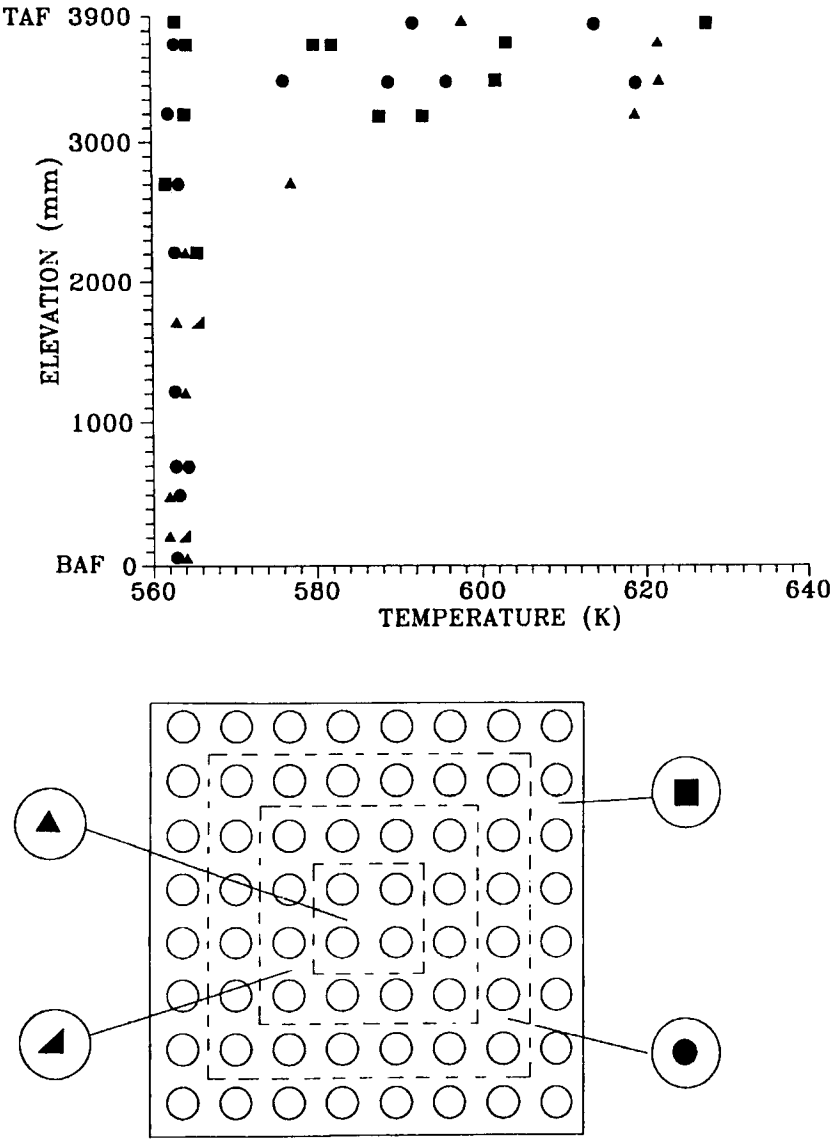

Figure 3.5. Axial and radial distribution of rod surface temperatures during intial CHF occurrence measured in the LOBI small break LOCA experiment BL-34.

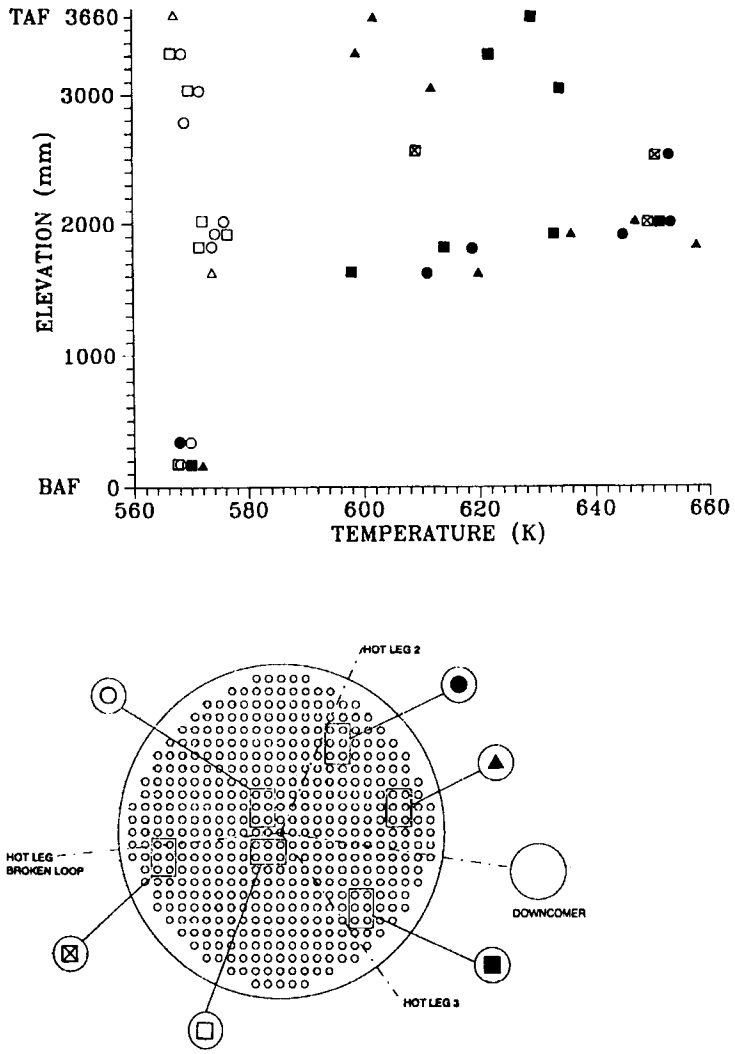

Figure 3.6. Axial and radial distribution of rod surface temperatures during initial CHF occurrence measured in the BETHSY small break LOCA experiment.

Three possible options are proposed to resolve the concerns of properly representing the thermalhydraulic/neutronic response to massive CHF occurrence.

(1) use subchannel codes to evaluate the spread of CHF occurrence in a core across a fuel cell or bundle;
(2) predict the *average* (not initial) CHF for a fuel cell or bundle and use this for predicting the fraction of fuel in dryout (this requires knowledge of the variation in flow conditions among fuel bundle/fuel cell);
(3) use subchannel codes and/or experimental data to relate the bundle/core drypatch fraction to heat flux beyond the initial CHF occurrence and use this in systems code calculations to predict the thermalhydraulic and neutronic response.

The choice of which option is appropriate depends on the application, the availability of relevant data and the type of subchannel and systems code.

3.7.3. Transient effects on CHF

3.7.3.1. Flow transient

During a LOCA or pump rundown scenario, the flow decay phase can frequently be characterized by $G = G_0 e^{-t/C1}$, during which time CHF will occur. The impact of the flow transient on CHF depends strongly on the flow decay constant C_1: This permits a subdivision of the transients into:

(i) slow transients, where the channel transit time is much smaller than the flow decay time constant C1. These are mild transients, which can be considered as pseudo-steady-state cases. Here, the CHF is assumed to be unaffected by the flow transient. For normal reactor flow conditions, the core transit time is roughly about 1 sec.

(ii) fast transients where the transit time is greater than the flow decay time constant C1. Here the CHF is expected to be affected noticeably by the transient and any effect due to AFD is considered secondary.

As a first order approximation, it may be assumed that for $1/G\ (dG/dt) < 0.1$ (i.e. a decay time constant C1 > 10 seconds) no effect of the transient on CHF is noticeable and the BLA heat flux (or any other methods which correctly account for upstream AFD) should be used. For a time constant C1 of 1 second or less, however, the BLA effect is no longer relevant as it is overshadowed by transient effects. It is generally assumed that the CHF is enhanced during fast transients but no reliable predictions are available. The assumption that $CHF_{transient} = CHF_{steady\ state}$ for the same instantaneous local flow conditions is frequently made.

3.7.3.2. Power transients

Power transients will also accompany a LOCA. The power transient can be either in the form of a power decay , or a power spike. The easiest methodology for representing the power change is by employing the "Lagrangian" approach. The similarity between the variation in upstream heat flux as experienced by a fluid parcel while travelling along a non-uniformly heated channel, and the change in heat flux experienced by a fluid particle during a power transient can be used in evaluating the impact of a power transient on CHF [see also Chang (1989)]. If the fluid is in the annular flow regime (void fractions >60%), a methodology similar to the BLA approach can be used, provided that the time a fluid particle sees a change in heat flux is transformed properly into an equivalent AFD. A previous study of axial flux spikes [Groeneveld (1975)] has shown that a BLA-type of approach can handle flux spikes with a magnitude of 2–3 times the average heat flux.

3.8. RECOMMENDATIONS AND FINAL REMARKS

(1) Based on the arguments presented in Sections 3.4-3.6, the CHF look-up table as presented in Appendix II is currently recommended for use as the reference prediction method for CHF in advanced water-cooled reactors. As an alternative for fuel bundles in which the rods are arranged in a triangular array, the WWER-based look-up table of Appendix III is recommended.

(2) For new bundle geometries, and in the absence of any relevant bundle CHF data, corrections for radial and axial flux shapes should be applied to account for differences between CHF values in tubes and bundle or bundle subchannels. These corrections can

best be obtained from a reliable subchannel code; without the complexity of a subchannel code, the method of applying correction factors based on element spacing, axial and radial flux distribution may be utilised.

(3) Supercritical water is currently being considered as a coolant medium for several Advanced Water Cooled Reactor concepts. The heat transfer characteristics of reactor cores cooled by supercritical water needs further investigation. Specifically the pseudo-CHF and post-CHF behaviour of supercritical water has received very little attention in the literature.

(4) Over 90% of the CHF literature is concerned with the prediction of initial CHF. There are currently no expressions for determining the average CHF or the spread of CHF available, even though this can be very important for predicting the thermalhydraulic and neutronic response to massive CHF occurrence during severe LOCAs. The methodology described in Section 3.7 may be used for evaluating the average CHF or the size of the drypatch.

(5) As shown in Figure 3.2 there exists currently a scarcity of CHF data at low flows/low qualities and at or high flows/high qualities. In addition relatively little is known of the effect of fast flow and power transients on CHF. Additional experiments are required to improve our knowledge of CHF in these areas.

REFERENCES TO CHAPTER 3

ADORNI, N., et al.. 1966, Heat Transfer Crisis and Pressure Drop with Steam-Water Mixtures: Experimental Data with 7-Rod Bundles at 50 and 70 kg/cm^2, CISE Report R170.

AKSAN, S.N., D'AURIA, F., FALUOMI, V., 1995, "A comparison and asessment of some chf prediction models used in thermalhydraulic systems codes", paper presented at First Research Coordination Mtg on Thermalhydraulic Relationships for Advanced Water-Cooled Reactors, IAEA-RC-574.

BAEK, W.-P., KIM, H.-C., CHANG, S.H., 1996, An Independent Assessment of Groeneveld et al.'s 1995 CHF Look up Table, Nuclear Engineering and Design.

BECKER, K.M., FLINTA, J., NYLUND, O., 1967, "Dynamic and static burnout studies for the full-scale Marviken fuel elements in the 8 MW Loop FRIGG" (Proceedings, Symp. on Two-Phase Flow Dynamics, Eindhoven, Netherlands), Vol. 1, 461–474.

BELSITO, S., D'AURIA, F., 1995, Comparison of Advanced Computer Codes in the Simulation of CHF Occurrence in the PKF Facility, Report on Expert Group Meetings on CHF and Post-CHF Heat Transfer, New Orleans, IAEA-CT-2991 and 2992.

BERGLES, A.E., 1977, Burnout in boiling heat transfer. Part II: Subcooled and low quality forced-convection systems, Nuclear Safety **18** 2 154–167.

BESTION, B., 1990, The physical closure laws in the CATHARE code, Nuclear Eng. Design **124** 229–245.

BEZRUKOV, Y.A., ASTACHOV, V.I., SALII, L.A., 1974, "Study of CHF in rod bundles for WWER type reactors", Proc. Thermophysical Mtg TF-74, Moscow (57–66).

BEZRUKOV, Y.A., ASTACHOV, V.I., BRANTOV, V.G., 1976, Experimental study and statistical analysis of CHF data for WWER type reactors, Teploenergetika **2** 80–82.

BOBKOV, V.P., VINOGRADOV, V.N., ZYATNINA, O.A., KOZINA, N.V., 1995, A method of evaluating the critical heat flux in channels and cells of arbitrary geometries, Thermal Engineering **42** 3 (221–231).

BOBKOV, V.P., VINOGRADOV, V.N., ZYATNINA, O.A., KOZINA, N.V., 1997, Considerations in describing burnout in rod bundles, Thermal Engineering **44** 3 (2–7).

BOWRING, R.W., 1967, HAMBO, A Computer Programme for the Subchannel Analysis and Burnout Characteristics of Rod Clusters, Part I. General Description, UKAEA Rep. AEEW-R524.

BURCK, E., HUFSCHMIDT, W., DE CLERQ, E., 1968, Der Einfluss Kuenstlicher Rauhigkeiten auf die Erhoehung der Kritischen Waermestromdichte von Wasser in Ringspalten bei erzweigener Konvektion, EUR 4040d.

CARVER, M.B., KITELEY, J.C., ZHOU, R.Q.N., JUNOP, S.V., 1993, Validation of ASSERT Subchannel Code for Standard and Non-Standard Geometries, ARD-TD-454P, 2nd Int. Seminar on Subchannel Analysis, EPRI, Palo Alto.

CHANG, S.H., LEE, K.W., GROENEVELD, D.C., 1989; Transient-effects modeling of critical heat flux, Nuclear Eng. Design **133** 51–57.

CHUN, T.H., HWANG, D.H., BAEK, W.P., CHANG, S.H., 1997, "Assessment of the look-up table method for bundle CHF predictions with a subchannel code" (Proc. ISSAC-4 Mtg Tokyo.

CERVOLANI, S., 1995, "Description and validation of ANTEO, an optimized PC code for the thermalhydraulic analysis of fuel element bundles" (Proc. 2nd Regional Mtg on Nuclear Energy in Central Europe, Portoroz, Slovenia).

CHENG, X., ERBACHER, F.J., 1997, this publication, Chapter 3.

COLLIER, J.G., 1972 and 1981, Convective Boiling and Condensation, McGraw-Hill, London.

D'AURIA, F., 1997, this publication, Figures 3.5 and 3.2.

DEBORTOLI, R.A., GREEN, S.J., LETOURNEAU, B.W., TROY, M., WEISS, A., 1958, Forced-Convection Heat Transfer Burnout Studies for Water in Rectangular Channels and Round Tubes at Pressures Above 500 Psia, Westinghouse Electric Corp. Rep. WAPD-188.

DOERFFER, S., GROENEVELD, D.C., SCHENK, J.R., 1996, "Experimental study of the effects of flow inserts on heat transfer and critical heat flux", (Proc. 4th Int. Conf. on Nuclear Engineering, New Orleans, Vol. 1 — Part A (41–49).

DOROSHCHUK, V.E., LEVITAN, L.L., LANTZMAN, F.P., Investigation into Burnout in Uniformly Heated Tubes, ASME Publication 75-WA/HT-22.

DURANT, W.S., TOWELL, R.H., MIRSHAK, S., 1965, "Improvement of Heat Transfer to Water Flowing in an Annulus by Roughening the Heated Wall", Chem. Engrg. Progress Symposium Series **6** 60 106–113.

FALUOMI, V., AKSAN, S.N., 1997, "Analysis and assessment of some selected CHF models as used in Relap5/Mod3 code", (Proceedings Fifth Int. Conf. on Nuclear Engineering (ICONE 5), Nice, France).

GASPARI, G.P., HASSID, A., VANOLI, G., 1969, "An experimental investigation on the influence of radial power distribution on critical heat flux in a nuclear rod cluster", (Proc. European Two-Phase Flow Group Mtg, Karlsruhe).

GASPARI, G.P., et al., 1968, Heat Transfer Crisis and Pressure Drop with Steam Water Mixtures: Further Experimental Data with Seven Rod Bundles, CISE Rep. R-208.

GROENEVELD, D.C., et al., 1996, The 1996 look-up table for critical heat flux in tubes, Nuclear Eng. Design **163** 1–23.

GROENEVELD, D.C., 1996, On the definition of critical heat flux margin, Nuclear Eng. Design **163** 245–247.

GROENEVELD, D.C., LEUNG, L.K.H., 1989, "Tabular approach to predicting critical heat flux and post-dryout heat transfer", Proc. 4th Int. Top. Mtg on Nuclear Reactors Thermalhydraulics, Karlsruhe), Vol 1, 109–114.

GROENEVELD, D.C., YOUSEF, W.W., 1980, "Spacing devices for nuclear fuel bundles: A survey of their effect on CHF, post-CHF heat transfer and pressure drop", (Proc. ANS/ASME/NRC Int. Top. Mtg on Nuclear Reactor Thermal-Hydraulics, Saratoga Springs), NUREG/CP-0014, Vol. 2, 1111–1130.

GROENEVELD, D.C., 1975, The Effect of Short Flux Spikes on the Dryout Power", Atomic Energy of Canada Ltd Rep. AECL–4927.

GROENEVELD, D.C., 1974, "The occurrence of upstream dryout in uniformly heated channels", (Proc. Fifth Int. Heat Transfer Conf.), Vol. IV (265–269).

GROENEVELD, D.C., 1972, The Thermal Behaviour of a Heated Surface at and Beyond Dryout", Atomic Energy of Canada Ltd Rep. AECL-4309.

GROENEVELD, D.C., SNOEK, C.W., 1986, "A comprehensive examination of heat transfer correlations suitable for reactor safety analysis", Multiphase Science and Technology, Volume II (181–274).

GROENEVELD, D.C., et al., 1986a, "Analytical and experimental studies in support of fuel channel critical power improvements", Proc. Canadian Nuclear Society Annual Mtg, Toronto.

GROENEVELD, D.C., et al., 1992, "CHF fluid-to-fluid modelling studies in three laboratories using different modelling fluids", (Proc. NURETH-5, Salt Lake City), Vol. 2, 531–538.

HERON, R.A., et al., 1969, Burnout Power and Pressure Drop Measurements on 12-ft., 7-rod Clusters Cooled by Freon-12 at Ispra, UKAEA Rep. AEEW-R655.

HETSRONI, G., 1982, "Handbook of multiphase systems", Hemisphere, McGraw-Hill.

HEWITT, G.F., HALL-TAYLOR, N.S., 1970, Annular Two-Phase Flow, Pergamon Press, Oxford.

HEWITT, G.F., KEARSEY, H.A., LACEY, P.M.C., PULLING, D.J., 1963, Burn-Out and Nucleation in Climbing Film Flow, UKAEA Rep. AERE-R437.

HSU, Y.Y., GRAHAM, R.W., 1976, Transport Processes in Boiling and Two Phase Systems, McGraw-Hill.

HUGHES, E.D., et al., 1974, A compilation of rod array critical heat flux data sources and information", Nuclear Engrg. & Design **30** 20–35.

JENSEN, A., MENNOV, G., 1974, Measurement of Burnout, Film Flow and Pressure Drop in a Concentric Annulus 3500 x 26 x 17 mm With a Heated Rod and Tube, European Two-Phase Flow Group Meeting, Harwell, UK.

KATTO, Y., 1994, Critical heat flux, Int. J Multiphase Flow **20** (53–90).

KIRILLOV, P.L., YUSHENKO, S.S., 1996, "Diameter effect on CHF", Second Research Coordination Meeting, IAEA Coordinated Research Program on Thermalhydraulic Relationships for Advanced Water-Cooled Reactors, Vienna, Austria.

KIRILLOV, P.L., BOBKOV., V.P., SMOGALEV, I.P., VINOGRADOV, V.N., 1996, Prediction of Critical Heat Flux in Channels Relevant to Water Cooled Reactors, IAEA Contract 8219R1.

KIRILLOV, P.L., BOBKOV. V.P., 1997, Working Material Related to the WWER-type Bundle CHF Look-up Table, Presented at the Third Research Coordination Meeting, Coordinated Research Program on Thermalhydraulic Relationships for Advanced Water-Cooled Reactors, Obninsk, Russia.

KITELEY, J.C., CARVER, M.B., LINER, Y., BROMLEY, B.P., MCCRACKEN, I.K., 1991, "ASSERT-IV thermalhydraulics subchannel analysis code simulation of dryout power and pressure drop in a horizontal 37-rod bundle fuel channel including the effect of pressure tube creep", Proc. 16th Annual CNA Nuclear Simulation Symp. St. John, New Brunswick.

KRUZHILIN, G.N., 1949, Experimental data on heat transfer boiling at natural convection", Izvestiya Akademii Nauk SSSR, Otdel Technik. Nauk **5** (701–702).

KUNSEMILLER, D.F., 1965, Multi-Rod, Forced Flow Transition and Film Boiling Measurements, General Electric Rep. GEAP-5073.

KUTATELADZE, S.S., 1952, Heat Transfer in Boiling and Condensation, USAEC Rep. AEC-tr-3770.

KUTATELADZE, S.S., BORISHANSKII, V.M., 1966, A Concise Encyclopedia of Heat Transfer, Pergamon Press.

KYMALAINEN, O., et al., 1993, "Heat flux distribution from a volumetrically heated pool with high Rayleigh number", (Proc. NURETH-6 Conf. Grenoble), Vol. 1 (47–53).

LAHEY, R.T., GONZALEZ-SANTOLO, J.M., 1977, "The effect of non-uniform axial heat flux on critical power", Paper C219/77 presented at the Inst. of Mech. Engineers Conf. on Heat and Fluid Flow in Water Reactor Safety, Manchester.

LAHEY, R.T., Jr., MOODY, F.J., 1977, The Thermal Hydraulics of a Boiling Water Nuclear Reactor, ANS Monograph.

LIN, W., LEE, C.H., PEI, B.S., 1989, An improved theoretical critical heat flux model for low quality flow", Nuclear Technol. **88** (294–306).

LEE, D.H., OBERTELLI, J.D., 1963, An Experimental Investigation of Forced Convection Boiling in High Pressure Water, UKAEA Rep. AEEW-R213.

LEUNG, L.K.H., 1997, AECL Report.

MACEK, J., 1998, Private Communication.

MCPHERSON, G.D., 1971, The Use of the Enthalpy Imbalance Number in Evaluating the Dryout Performance of Fuel Bundles, AECL Rep. AECL-3968.

NORMAN, W.S., MCINTYRE, V., 1960, Heat transfer and liquid film on a vertical surface, Trans. Inst. Chem. Engineers **38** 301–307.

PARK, H., DHIR, V. K., et al., 1994, Effect of external cooling on the thermal behavior of a boiling water reactor vessel lower head, Nuclear Technol. V. **108** 2 266–282.

POLOMIK, E.E., 1967, Transition Boiling, Heat Transfer Program, Final Summary Report on Program for Feb. 63–Oct. 67, General Electric Report GFAP-5563.

ROWE, D.S., 1971, COBRA III, A Digital Computer Program for Steady State and Transient Thermal-Hydraulics Analysis of Rod-Bundle Nuclear Fuel Elements, Battelle-Northwest Report BNWL-B-82.

SCHENK, J.R., GROENEVELD, D.C., 1990, "Measurement of thermalhydraulic parameters inside multi-element bundles", Proc. Int. Symp. on Multi-Phase Flow, Miami.

SMITH, R.A., 1986, Boiling Inside Tubes: Critical Heat Flux for Upward Flow in Uniformly Heated Tubes, ESDU Data Item No. 86032, Engineering Science Data Unit International Ltd, London.

SULATSKI, A.A., EFIMOV, V.K., GRANOVSKY, V.S., 1997, "Boiling crisis at the outer surface of WWER vessel", Proc. Int. Symp. on the Physics of Heat Transfer in Boiling and Condensation, Moscow (263–268).

TAITEL, Y., DUKLER, A.E., 1975, A Model for Predicting Flow Regime Transitions in Horizontal and Near Horizontal Gas/Liquid Flow, ASME 750WA/HT829 (1975); AIChE J. **22** (1976) 47855.

TIPPETS, F.E., 1962, "Critical Heat Fluxes and Flow Patterns in High Pressure Boiling Water Flows", ASME Paper 62-WA-162 presented at the Winter Annual Meeting of the ASME, New York.

TODREAS, N.E., ROHSENOW, W.M., 1965, The Effect of Non-uniform Axial Heat Flux Distribution, Rep. 9843–37, M.I.T. Dept. of Mech. Engineering.

TONG, L.S., HEWITT, G.F., 1972, Overall Viewpoint of Flow Boiling CHF Mechanisms, ASME paper 72-HT-54.

TONG, L.S., 1972, Boiling Crisis and Critical Heat Flux, USAEC Rep. TID-25887.

TONG, L.S., WEISMAN, J., 1996, Thermal Analysis of Pressurized Water Reactors, Third Edn, American Nuclear Society.

TONG, L.S., 1965, Boiling Heat Transfer and Two-Phase Flow, John Wiley & Sons.

TOWELL, R.H., 1965, Effect of Spacing on Heat Transfer Burnout in Rod Bundles, Report DP-1013.

ULRYCH, G., 1993, "CHF table applications in KWV PWR design", Paper presented at the Int. Workshop on CHF Fundamentals — CHF Table Improvements, Braunschweig.

WATERS, E.O., FITZSIMMONS, D.E., 1963 DNB varies with rod spacing in 19-rod bundles, Nucleonics (96–101).

WEAVER, W.L., RIEMKE, R.A., WAGNER, R.J., JOHNSON, G.W., 1991, "The RELAP5/MOD3 code for PWR safety analysis", (Proc. NURETH-4". 4th Int. Top. Mtg on Nuclear Reactor Thermalhydraulics, Karlsruhe", Vol. 2 (1221–1226).

WEISMAN, J., BOWRING, R.W., 1975, Methods for detailed thermal and hydraulic analysis of water-cooled reactors, Nuclear Science Engineer. **57** (255–276).

WEISMAN, J., 1992, The current status of theoretically based approaches to the prediction of the critical heat flux in flow boiling, Nuclear Technol. **99** (1–21).

WEISMAN, J., PEI, B.S., 1983, Prediction of critical heat flux in flow boiling at low quality conditions, Int. J. Heat Mass Transfer **26** (1463).

WEISMAN, J., YING, S.H., 1985, A theoretical based critical heat flux prediction for rod bundles, Nucl. Eng. Design **85** (239–250).

YING, S.H., WEISMAN, J., 1986, Prediction of critical heat flux in flow boiling at intermediate qualities, Int. J. Heat Mass Transfer **29** (1639).

WONG, Y.L., GROENEVELD, D.C., CHENG, S.C., 1990, CHF predictions in horizontal tubes, Int . J. Multiphase Flow **16** (123).

ZUBER, N., 1959, Hydrodynamic Aspects of Boiling Heat Transfer, Atomic Energy Commission Report AECU-4439.